

# An Investigation of the NO/H<sub>2</sub>/O<sub>2</sub> (Lean-deNO<sub>x</sub>) Reaction on a Highly Active and Selective Pt/La<sub>0.5</sub>Ce<sub>0.5</sub>MnO<sub>3</sub> Catalyst

C. N. Costa,\* V. N. Stathopoulos,† V. C. Belessi,† and A. M. Efsthathiou\*,<sup>1</sup>

\*Department of Chemistry, University of Cyprus, P.O. Box 20537, CY 1678 Nicosia, Cyprus; and †Department of Chemistry, University of Ioannina, Ioannina 45 110, Greece

Received August 7, 2000; revised October 27, 2000; accepted October 30, 2000; published online January 12, 2001

The NO/H<sub>2</sub>/O<sub>2</sub> reaction has been studied under lean-burn conditions in the 100–400°C range over 0.1 wt% Pt supported on La<sub>0.5</sub>Ce<sub>0.5</sub>MnO<sub>3</sub> (mixed oxide containing LaMnO<sub>3</sub>, CeO<sub>2</sub>, and MnO<sub>2</sub> phases). For a critical comparison, 0.1 wt% Pt was supported on  $\gamma$ -Al<sub>2</sub>O<sub>3</sub> and tested under the same reaction conditions. The maximum in the NO conversion has been observed at 140°C (74% conversion) for the Pt/La<sub>0.5</sub>Ce<sub>0.5</sub>MnO<sub>3</sub> and at 125°C (66% conversion) for the Pt/ $\gamma$ -Al<sub>2</sub>O<sub>3</sub> catalyst using a GHSV of 80,000 h<sup>-1</sup>. Addition of 5% H<sub>2</sub>O in the feed stream influenced the performance of the catalyst in a positive way. In particular, it widened the operating temperature window of the catalyst above 200°C with appreciable NO conversion and had no negative effect on the stability of the catalyst for a 20-h run on reaction stream. Remarkable N<sub>2</sub> selectivity values in the 80–90% range have been observed on the Pt/La<sub>0.5</sub>Ce<sub>0.5</sub>MnO<sub>3</sub> catalyst in the 100–200°C range either in the absence or in the presence of water in the feed stream. This result is reported for the first time for the NO/H<sub>2</sub>/O<sub>2</sub> lean-deNO<sub>x</sub> reaction at least on Pt-based catalysts. A maximum specific integral reaction rate of 397  $\mu$ mol of N<sub>2</sub>/s.g of Pt metal was measured at 140°C during reaction with 0.25% NO/1% H<sub>2</sub>/5% O<sub>2</sub>/5% H<sub>2</sub>O/He gas mixture on the 0.1 wt% Pt/La<sub>0.5</sub>Ce<sub>0.5</sub>MnO<sub>3</sub> catalyst. This value was found to be higher by 40% than that observed on the 0.1 wt% Pt/ $\gamma$ -Al<sub>2</sub>O<sub>3</sub> catalyst at 125°C, and it is the highest value ever reported in the 100–200°C range. A TOF value of 0.49 s<sup>-1</sup> was calculated at 140°C for the Pt/La<sub>0.5</sub>Ce<sub>0.5</sub>MnO<sub>3</sub> catalyst. Temperature-programmed desorption (TPD) of NO and transient titration experiments of the catalyst surface following reaction have revealed important information concerning several mechanistic steps of the present catalytic system. A hydrogen-assisted NO dissociation step and a nitrogen-assisted mechanism for N<sub>2</sub> and N<sub>2</sub>O formation are proposed to explain all the transient experiments performed in a satisfactory manner.

© 2001 Academic Press

**Key Words:** lean de-NO<sub>x</sub>; NO reduction; NO TPD; perovskites.

## 1. INTRODUCTION

Much research concerning the selective catalytic reduction (SCR) of NO by NH<sub>3</sub> and hydrocarbons under net

<sup>1</sup> To whom correspondence should be addressed. Fax: (+3572)-339060. E-mail: [efstath@ucy.ac.cy](mailto:efstath@ucy.ac.cy).

oxidizing conditions has been undertaken and reported in the literature as recently reviewed (1–3). Today's great concern about the increasing emissions of carbon dioxide to the atmosphere and the problems faced resulting from the use of NH<sub>3</sub> as a reducing agent (4) lead to a demand for finding appropriate non-carbon-containing reducing molecules for the catalytic removal of NO from combustion exhaust streams. Hydrogen is one of the gases present in the exhaust stream of automobiles and has been reported to be very effective as a reducing agent for the NO/H<sub>2</sub> reaction (5–16). Hydrogen could also be used to reduce NO<sub>x</sub> emissions of stationary sources. However, only a few attempts have been reported for the reduction of NO by H<sub>2</sub> under oxygen-rich conditions (17–20) because H<sub>2</sub> can be easily consumed by reacting with O<sub>2</sub> to form water under the applied reaction conditions (21, 22).

Supported platinum catalysts have been found to be the most active for the NO/H<sub>2</sub>/O<sub>2</sub> lean-NO<sub>x</sub> reaction at low temperatures ( $T < 200^\circ\text{C}$ ) (17–20). Yokota *et al.* (20) have reported catalytic results on the NO reduction with H<sub>2</sub> in the presence of O<sub>2</sub> over the Pt–Mo–Na/SiO<sub>2</sub> catalyst, while Frank *et al.* (17) reported kinetic results of the NO/H<sub>2</sub>/O<sub>2</sub> reaction on the Pt–Mo–Co/ $\alpha$ -Al<sub>2</sub>O<sub>3</sub> catalyst. The latter two catalyst formulations were found to produce substantially lower amounts of N<sub>2</sub>O (N<sub>2</sub> selectivity at about 75%) as compared to conventional supported Pt catalysts (e.g., Pt/Al<sub>2</sub>O<sub>3</sub>, Pt/SiO<sub>2</sub>) which are known to present lower N<sub>2</sub> selectivity values ( $S_{\text{N}_2} = 40\text{--}50\%$ ). On the other hand, it was reported (20) that the Pt–Mo–Na/SiO<sub>2</sub> catalyst shows a relatively low stability under lean-burn conditions in the presence of water.

In our laboratory we have initiated a research program concerning the use of certain perovskite-type materials as potential catalysts or supports of active metals for the selective reduction of NO under oxygen-rich conditions. It was found that La<sub>0.5</sub>Ce<sub>x</sub>Sr<sub>0.5-x</sub>MnO<sub>3</sub> solids present a relatively low catalytic activity and high selectivity toward N<sub>2</sub> formation for the NO/H<sub>2</sub>/O<sub>2</sub> reaction in the 250–500°C range. However, the combination of such a selective system with a very small amount of Pt (0.1 wt%) results in a catalyst

composition of high activity and N<sub>2</sub> selectivity in the 100–200°C range. This catalytic system exhibits also a high stability in the presence of 5% H<sub>2</sub>O in the feed stream. These features suggest that the present catalyst may be an important candidate for low-temperature lean-deNO<sub>x</sub> applications.

The present work concerns catalytic and transient reactivity studies on a 0.1 wt% Pt/La<sub>0.5</sub>Ce<sub>0.5</sub>MnO<sub>3</sub> catalyst for both the NO/H<sub>2</sub>/O<sub>2</sub> and NO/H<sub>2</sub> reactions. The same studies were also conducted on a 0.1 wt% Pt/Al<sub>2</sub>O<sub>3</sub> catalyst for a critical comparison. Transient surface reactivity studies have been carried out on both metal-supported catalysts and the corresponding supports in order to obtain fundamental information about the nature and reactivity of intermediate species involved in the mechanism of the NO/H<sub>2</sub>/O<sub>2</sub> reaction. The transient studies involved (a) temperature-programmed desorption (TPD) of NO, (b) temperature-programmed surface reaction (TPSR) in He flow, and (c) TPSR in H<sub>2</sub>/He flow following the NO/H<sub>2</sub>/O<sub>2</sub> reaction. The latter two kinds of transient experiments allowed for the estimation of the surface coverage of molecularly adsorbed NO and that of total N-containing intermediate species formed under NO/H<sub>2</sub>/O<sub>2</sub> reaction conditions. In addition, the surface reactivity of these species toward He and H<sub>2</sub>/He treatment has been studied. The transient experiments performed support the view for a hydrogen-assisted dissociation step of NO and a nitrogen-assisted reduction mechanism of NO to N<sub>2</sub> and N<sub>2</sub>O gas products.

## 2. EXPERIMENTAL

### 2.1. Catalysts Preparation

The La<sub>0.5</sub>Ce<sub>x</sub>Sr<sub>0.5-x</sub>MnO<sub>3</sub> solids were prepared using the ceramic method as follows: calculated amounts of La(NO<sub>3</sub>)<sub>3</sub>·6H<sub>2</sub>O (Merck), Sr(NO<sub>3</sub>)<sub>2</sub> (Ferak), Mn(NO<sub>3</sub>)<sub>3</sub>·9H<sub>2</sub>O (Merck), and CeO<sub>2</sub> (Aldrich) were mixed thoroughly in an agate mortar and heated slowly to 400°C for nitrate decomposition. At the end of this step (no visible NO<sub>2</sub> fumes), the system was further heated for 4 h at 900°C at 1 atm. The mixture was then removed from the furnace, cooled, and after grinding was heated again for another 4 h at 1050°C. The sample was then slowly cooled to room temperature and stored for further use. It is mentioned that the notation La<sub>0.5</sub>Ce<sub>x</sub>Sr<sub>0.5-x</sub>MnO<sub>3</sub> indicates just the nominal composition of the solids. This has nothing to do with particular crystal phases existing in each sample.

The metal-supported catalysts (0.1 wt% Pt/La<sub>0.5</sub>Ce<sub>0.5</sub>MnO<sub>3</sub> and 0.1 wt% Pt/Al<sub>2</sub>O<sub>3</sub>) were prepared by the incipient wetness impregnation method using the H<sub>2</sub>Pt(IV)Cl<sub>6</sub> (Aldrich) precursor for both catalysts. The γ-Al<sub>2</sub>O<sub>3</sub> support was supplied by Aldrich (standard grade, 150 mesh). After impregnation and drying (overnight at ~120°C), the catalyst sample was calcined in air at 400°C for 2 h prior to use.

### 2.2. Catalysts Characterization

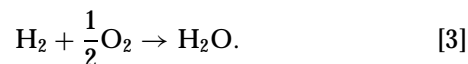
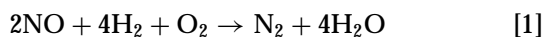
**Surface area and metal dispersion measurements.** The specific surface area of the La<sub>0.5</sub>Ce<sub>x</sub>Sr<sub>0.5-x</sub>MnO<sub>3</sub> and γ-Al<sub>2</sub>O<sub>3</sub> solids was checked by N<sub>2</sub> adsorption at 77 K (BET method) using a multipoint Fisons Sorptly 1900 System. Metal dispersions of the catalysts were determined by H<sub>2</sub> chemisorption at room temperature followed by TPD in He flow.

**XRD analysis.** The crystal structure of the prepared La<sub>0.5</sub>Ce<sub>x</sub>Sr<sub>0.5-x</sub>MnO<sub>3</sub> solids was checked by XRD measurements using a SIEMENS Diffract 500 system employing CuKα radiation (λ = 1.5418 Å).

### 2.3. Catalytic and Transient Studies

The flow system used for conducting catalytic measurements for the NO/H<sub>2</sub>/O<sub>2</sub> (lean-deNO<sub>x</sub>) reaction at 1 atm total pressure consisted of a flow measuring and control system (MKS Instruments, Model 247C), mixing chambers, a quartz fixed-bed microreactor (2 ml nominal volume), and a GC-MS analysis system. The flow system, the microreactor, and the analysis system used have been recently described in detail (23). The feed stream consisting of 0.25% NO, 1.0% H<sub>2</sub>, 5% O<sub>2</sub>, and He as balance gas was used in all experiments. The amount of supported Pt catalyst sample used for the catalytic experiments was 0.15 g and the total flow rate was 100 cm<sup>3</sup> (STP)/min, resulting in a GHSV of about 80,000 h<sup>-1</sup>. For the experiments to study the effects of H<sub>2</sub>O in the feed stream on the NO conversion, a feed gas mixture of about 5 mol% H<sub>2</sub>O/He was prepared by flowing He through a deionized water saturator held at 35°C (±1°C). The exit stream was then mixed with NO/He, H<sub>2</sub>/He, and O<sub>2</sub>/He gas mixtures at the appropriate mass flow rates in order to produce the desired feed gas composition. Reaction rates (kinetic or integral) were calculated using the relationship Rate (mol · g<sup>-1</sup> · s<sup>-1</sup>) = N<sub>T</sub>y<sub>i</sub>/W · N<sub>T</sub> (mol/s) is the total molar exit flow rate, y<sub>i</sub> is the molar fraction of component *i* (e.g., N<sub>2</sub>) expressed in ppm × 10<sup>-6</sup>, and *W* is the weight of the catalyst (g). Reaction turnover frequencies (TOF, s<sup>-1</sup>) were calculated on the basis of the exposed Pt atoms (4.6 μmol of Pt/g<sub>cat</sub>).

For the present catalytic reaction system, H<sub>2</sub> reacts with NO and O<sub>2</sub> on the basis of the following competitive reaction scheme:



The only N-containing product species formed in the present catalytic reaction system were N<sub>2</sub> and N<sub>2</sub>O. The

TABLE 1

Description of Sequential Step Changes of Gas Flow during Temperature-Programmed Desorption (TPD) and Surface Reaction (TPSR) Experiments Performed on  $\text{La}_{0.5}\text{Ce}_{0.5}\text{MnO}_3$ ,  $\gamma\text{-Al}_2\text{O}_3$ , 0.1% Pt/ $\text{La}_{0.5}\text{Ce}_{0.5}\text{MnO}_3$ , and 0.1% Pt/ $\text{Al}_2\text{O}_3$  Catalysts

Experiment	Sequence of step changes of gas flow over the catalyst sample
A	0.5% NO/He (room temperature, 20 min) → He (5 min, room temperature) → <u>TPD in He</u>
B	0.25% NO/1.0% H <sub>2</sub> /5% O <sub>2</sub> (140°C, 30 min) → cool quickly to room temperature in reaction mixture → He (5 min, 30°C) → <u>TPSR in He</u>
C	0.25% NO/1.0% H <sub>2</sub> /5% O <sub>2</sub> (140°C, 30 min) → cool quickly to room temperature in reaction mixture → He (5 min, 30°C) → <u>TPSR in 10% H<sub>2</sub>/He</u>

selectivity,  $\alpha$ , for reduction of NO by H<sub>2</sub> to N<sub>2</sub>, e.g., the ratio of the consumption rate of H<sub>2</sub> for reaction [1] to the total consumption rate of H<sub>2</sub> (reactions [1]–[3]), is calculated on the basis of the following:

$$\alpha(\%) = \frac{0.5 y_{\text{NO}}^f X_{\text{NO}}}{y_{\text{H}_2}^f X_{\text{H}_2}} S_{\text{N}_2} \times 100. \quad [4]$$

In Eq. [4],  $y_{\text{NO}}^f$  and  $y_{\text{H}_2}^f$  are the feed molar fractions of NO and H<sub>2</sub>, respectively,  $X_{\text{NO}}$  and  $X_{\text{H}_2}$  are the NO and H<sub>2</sub> conversions, respectively, and  $S_{\text{N}_2}$  is the selectivity of the reaction to N<sub>2</sub> gas product. The value of 0.5 is the stoichiometric ratio of NO to H<sub>2</sub> appeared in reaction [1].

Temperature-programmed desorption (TPD) and surface reaction (TPSR) experiments were conducted in a specially designed flow system that has been recently described (23). For transient experiments, the amount of catalyst sample used was 0.15–0.2 g. The total flow rate was kept constant at 30 cm<sup>3</sup>(STP)/min. Chemical analysis of the gas effluent stream of reactor during transients was done with an *online* quadrupole mass spectrometer (Omnistar, Balzers) equipped with a fast response inlet capillary/leak valve (SVI 050, Balzers) and data acquisition systems. The gaseous responses obtained by mass spectrometry were calibrated against standard mixtures. The mass numbers ( $m/z$ ) 15, 28, 30, 32, 44, and 46 were used for NH<sub>3</sub>, N<sub>2</sub>, NO, O<sub>2</sub>, N<sub>2</sub>O, and NO<sub>2</sub>, respectively.

Before any measurements were taken, the support materials were pretreated in 5% O<sub>2</sub>/He for 2 h at 500°C, while the supported Pt catalysts were pretreated at 400°C for 2 h followed by treatment with a 10% H<sub>2</sub>/He gas mixture at 300°C for 2 h. The feed was then switched to pure He at 500 or 300°C, respectively, for 15 min and the reactor was cooled to the appropriate temperature of the experiment to be followed. Table 1 describes the necessary sequence of steps performed for each kind of transient experiments presented in this work. The underlined step is that during

of which measurements by online mass spectrometry were recorded.

### 3. RESULTS

#### 3.1. Catalysts Characterization

**BET surface area measurements.** The specific surface areas (*BET*, m<sup>2</sup>/g) of the  $\text{La}_{0.5}\text{Ce}_x\text{Sr}_{0.5-x}\text{MnO}_3$  solids were evaluated on the basis of results of the measured nitrogen isotherms at 77 K. The *BET* areas were found to be in the 3–4 m<sup>2</sup>/g range. In the case of  $\gamma\text{-Al}_2\text{O}_3$ , the *BET* area was found to be 155 m<sup>2</sup>/g. Before any measurements were taken, the sample was outgassed at 250°C under vacuum ( $P \approx 1.3 \times 10^{-3}$  mbar) overnight.

**X-ray diffraction studies.** The crystal phase composition of the  $\text{La}_{0.5}\text{Ce}_x\text{Sr}_{0.5-x}\text{MnO}_3$  solids as determined by XRD with reference to ASTM standards is shown in Table 2. The main crystal phases detected are the  $\text{LaMnO}_3$  and  $\text{SrMnO}_{3-x}$  of perovskite structure and the oxidic phases of CeO<sub>2</sub> and MnO<sub>2</sub>.

**Metal dispersion.** The dispersion of platinum metal for each of the 0.1 wt% Pt/ $\text{Al}_2\text{O}_3$  and 0.1 wt% Pt/ $\text{La}_{0.5}\text{Ce}_{0.5}\text{MnO}_3$  catalysts was found to be about 90% (4.6  $\mu\text{mol}$  of Pt<sub>s</sub>/g<sub>cat</sub>) on the basis of H<sub>2</sub> chemisorption (10% H<sub>2</sub>/He,  $T = 20^\circ\text{C}$ ,  $t = 30$  min,  $q = 30$  cm<sup>3</sup>/min) followed by TPD in He flow. This value gives an average particle size of about 12 Å. It is noted that no H<sub>2</sub> spillover effect was found under the hydrogen chemisorption conditions applied.

#### 3.2. Catalysts Performance and Stability with Time on Stream for the NO/H<sub>2</sub>/O<sub>2</sub> Reaction

**3.2.1.  $\text{La}_{0.5}\text{Ce}_x\text{Sr}_{0.5-x}\text{MnO}_3$  solids.** The four solids of the  $\text{La}_{0.5}\text{Ce}_x\text{Sr}_{0.5-x}\text{MnO}_3$  series prepared (Table 2) were tested for the NO/H<sub>2</sub>/O<sub>2</sub> reaction in the 200–500°C range. The  $\text{La}_{0.5}\text{Ce}_{0.5}\text{MnO}_3$  solid exhibits the best catalytic performance in terms of NO conversion and N<sub>2</sub> selectivity as shown in Table 3. In this table,  $T_{\text{max}}$  is the temperature at which a maximum in NO conversion was observed. N<sub>2</sub> selectivity values are in the 83–92% range (at  $T = 350\text{--}400^\circ\text{C}$ ), while the NO conversion varies between 20 and 24% under the indicated reaction conditions. The  $\text{La}_{0.5}\text{Ce}_{0.5}\text{MnO}_3$  solid

TABLE 2

Prepared  $\text{La}_{0.5}\text{Ce}_x\text{Sr}_{0.5-x}\text{MnO}_3$  Solids and Crystal Phases Detected by XRD

Solid composition	Crystal phases
$\text{La}_{0.5}\text{Ce}_{0.5}\text{MnO}_3$	$\text{LaMnO}_3/\text{MnO}_2/\text{CeO}_2/\text{La}(\text{OH})_3^*$
$\text{La}_{0.5}\text{Sr}_{0.5}\text{MnO}_3$	$\text{LaMnO}_3/\text{SrMnO}_{3-x}/\text{MnO}_2/\text{La}(\text{OH})_3^*$
$\text{La}_{0.5}\text{Sr}_{0.3}\text{Ce}_{0.2}\text{MnO}_3$	$\text{LaMnO}_3/\text{MnO}_2/\text{CeO}_2/\text{SrMnO}_{3-x}/\text{La}(\text{OH})_3^*$
$\text{La}_{0.5}\text{Sr}_{0.2}\text{Ce}_{0.3}\text{MnO}_3$	$\text{LaMnO}_3/\text{MnO}_2/\text{CeO}_2/\text{La}(\text{OH})_3^*/\text{SrMnO}_{3-x}^*$

\*Traces

TABLE 3

Catalytic Activity of the La<sub>0.5</sub>Ce<sub>x</sub>Sr<sub>0.5-x</sub>MnO<sub>3</sub> Solids for the NO/H<sub>2</sub>/O<sub>2</sub> Reaction<sup>a</sup>

Support	T <sub>max</sub> (°C)	X <sub>NO</sub> (%)	S <sub>N<sub>2</sub></sub> (%)
La <sub>0.5</sub> Sr <sub>0.5</sub> MnO <sub>3</sub>	400	20.8	82.9
La <sub>0.5</sub> Ce <sub>0.2</sub> Sr <sub>0.3</sub> MnO <sub>3</sub>	400	23.7	91.6
La <sub>0.5</sub> Sr <sub>0.2</sub> Ce <sub>0.3</sub> MnO <sub>3</sub>	350	19.9	89.2
La <sub>0.5</sub> Ce <sub>0.5</sub> MnO <sub>3</sub>	400	24.3	92.2

<sup>a</sup> W = 0.2 g. Feed conditions: 0.25% NO, 1% H<sub>2</sub>, 5% O<sub>2</sub>, He as balance gas; GHSV = 30,000 h<sup>-1</sup>.

was chosen as a support for the preparation of the 0.1 wt% Pt/La<sub>0.5</sub>Ce<sub>0.5</sub>MnO<sub>3</sub> catalyst on the basis of the results of Table 3.

**3.2.2. Pt/La<sub>0.5</sub>Ce<sub>0.5</sub>MnO<sub>3</sub> and Pt/Al<sub>2</sub>O<sub>3</sub> catalysts.** The catalytic behavior of the 0.1 wt% Pt/La<sub>0.5</sub>Ce<sub>0.5</sub>MnO<sub>3</sub> solid as a function of reaction temperature for the reduction of NO by H<sub>2</sub> in the presence of 5% O<sub>2</sub> is presented in Figs. 1 and 2. Catalytic results are given in terms of NO conversion (X<sub>NO</sub>, %) and N<sub>2</sub> selectivity (S<sub>N<sub>2</sub></sub>, %) in the 100–400°C range (Fig. 1a). The temperature of 400°C was the highest investigated in order to avoid sintering of Pt metal.

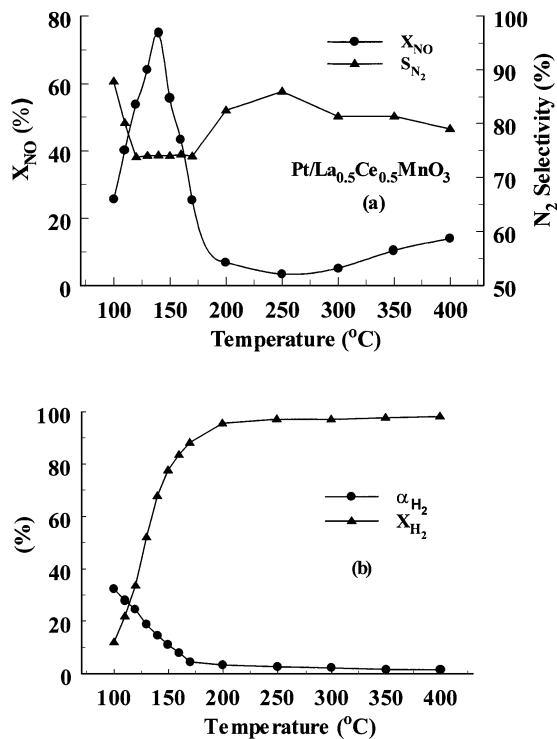


FIG. 1. Temperature profiles of (a) the NO conversion, X<sub>NO</sub> (●), and N<sub>2</sub> selectivity, S<sub>N<sub>2</sub></sub> (▲), and (b) the H<sub>2</sub> conversion, X<sub>H<sub>2</sub></sub> (▲), and H<sub>2</sub> reaction selectivity, α<sub>H<sub>2</sub></sub> (●), of the NO/H<sub>2</sub>/O<sub>2</sub> “lean-NO<sub>x</sub>” reaction on the 0.1 wt% Pt/La<sub>0.5</sub>Ce<sub>0.5</sub>MnO<sub>3</sub> catalyst. Reaction conditions: H<sub>2</sub> = 1.0%, NO = 0.25%, O<sub>2</sub> = 5%, W = 0.15 g, GHSV = 80,000 h<sup>-1</sup>.

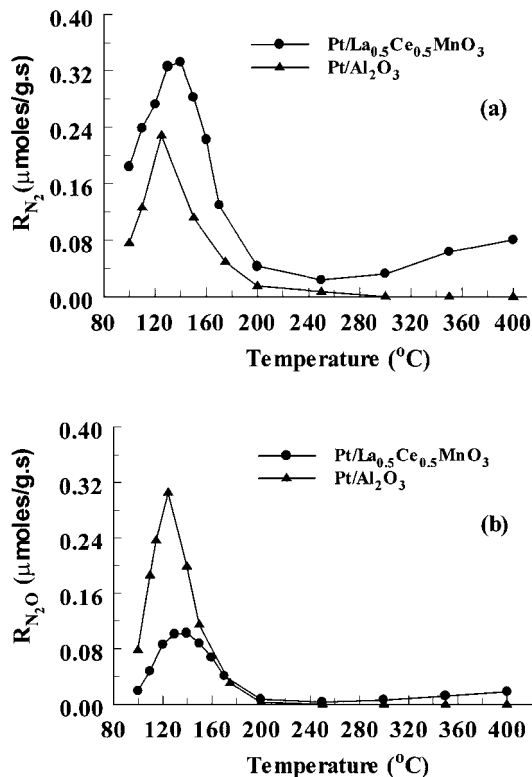


FIG. 2. Temperature profiles of (a) N<sub>2</sub> and (b) N<sub>2</sub>O integral production rates for the NO/H<sub>2</sub>/O<sub>2</sub> “lean-NO<sub>x</sub>” reaction on the 0.1 wt% Pt/La<sub>0.5</sub>Ce<sub>0.5</sub>MnO<sub>3</sub> (●) and 0.1 wt% Pt/Al<sub>2</sub>O<sub>3</sub> (▲) catalysts. Reaction conditions: H<sub>2</sub> = 1.0%, NO = 0.25%, O<sub>2</sub> = 5%, W = 0.15 g, GHSV = 80,000 h<sup>-1</sup>.

The X<sub>NO</sub> behavior of the catalyst can be distinguished in three different temperature ranges. In the 100–160°C low-temperature range the catalyst presents high catalytic activity (X<sub>NO</sub> > 20%) with a maximum conversion of 75% at 140°C. Between 200 and 300°C the activity of the catalyst is very small, while in the 300–400°C high-temperature range the NO conversion is between 5 and 15%. The latter behavior is mostly due to the activity of support itself as illustrated by the catalytic results shown in Table 3. The N<sub>2</sub> selectivity behavior of the Pt/La<sub>0.5</sub>Ce<sub>0.5</sub>MnO<sub>3</sub> catalyst is as follows. The catalyst is highly selective toward N<sub>2</sub> formation with selectivity values in the 75–87% range. The N<sub>2</sub> selectivity remains practically unchanged in the 120–160°C range (S<sub>N<sub>2</sub></sub> = 75%), while it increases to 80–87% at temperatures higher than 160°C and lower than 120°C.

Figure 1b presents the temperature profile of H<sub>2</sub> conversion (X<sub>H<sub>2</sub></sub>, %) for the corresponding experiments of Fig. 1a, and the corresponding profile of the H<sub>2</sub> selectivity of reaction parameter (α<sub>H<sub>2</sub></sub>, %) given by Eq. [4]. The H<sub>2</sub> conversion increases with reaction temperature, where at 250°C the value obtained is found to be about 95% and increases only slightly in the 250–400°C range. This temperature profile of H<sub>2</sub> conversion is totally different than that of NO conversion as seen in Fig. 1a. As the temperature of the

reaction increases, the percentage of  $H_2$  used for the desired reaction [1] decreases due to the  $H_2$  combustion reaction [3]. It will be shown later that the rate of  $H_2$  combustion is significantly higher than the rate of  $NO/H_2/O_2$  reaction, and this explains the temperature profile of  $H_2$  reaction selectivity (Fig. 1b).

Figure 2 presents comparative results concerning the integral rates per gram of catalyst of  $N_2$  (Fig. 2a) and  $N_2O$  (Fig. 2b) formation among the 0.1 wt%  $Pt/La_{0.5}Ce_{0.5}MnO_3$  and 0.1 wt%  $Pt/Al_2O_3$  catalysts in the 100–400°C range. As shown in Fig. 2a, the two catalysts present profiles similar in quality in the 100–200°C range, where the  $Pt/La_{0.5}Ce_{0.5}MnO_3$  exhibits significantly higher rates of  $N_2$  formation than the  $Pt/Al_2O_3$  catalyst. There is practically no activity of  $Pt/Al_2O_3$  in the 250–400°C range, a behavior different than that observed on the  $Pt/La_{0.5}Ce_{0.5}MnO_3$  catalyst. For the latter case, an increasing reaction rate is observed in the 250–400°C range, where at 400°C a rate similar to that obtained at 100°C was estimated. As clearly shown in Fig. 2b, the  $Pt/Al_2O_3$  catalyst presents significantly higher rates of  $N_2O$  production in the 100–140°C range than the  $Pt/La_{0.5}Ce_{0.5}MnO_3$  catalyst does. In particular, at  $T_{max} = 140^\circ C$  the rate of  $N_2O$  formation on the  $Pt/Al_2O_3$  is 3 times higher than that obtained on the  $Pt/La_{0.5}Ce_{0.5}MnO_3$  catalyst. Thus, it is apparent from the results of Fig. 2 that the use of  $La_{0.5}Ce_{0.5}MnO_3$  solid instead of  $\gamma-Al_2O_3$  as support of Pt metal has significantly improved the  $N_2$  selectivity of Pt metal in the 100–200°C low-temperature range.

It was interesting to study the rate of NO decomposition in the 200–400°C range where the  $H_2$  conversion is very high (Fig. 1b). After using a 0.25% NO/He mixture over the  $Pt/La_{0.5}Ce_{0.5}MnO_3$  catalyst, it was found that a maximum rate of 0.022  $\mu mol$  of  $N_2/g.s$  is obtained at 350°C. At 200°C a rate of 0.004  $\mu mol$  of  $N_2/g.s$  was estimated. These results clearly indicate that the decomposition reaction of NO itself contributes only to a small extent in the case where low concentrations of hydrogen are present in the feed stream. It is noted that the  $N_2$  selectivity of the NO/He reaction was found to be in the 85–98% range at temperatures between 200 and 400°C.

The catalytic behavior of the  $Pt/La_{0.5}Ce_{0.5}MnO_3$  solid was also studied in the presence of 5 mol% water in the feed stream containing 0.25 mol% NO, 1.0 mol%  $H_2$ , 5 mol%  $O_2$ , and He as balance gas. The temperature profile obtained is presented in Fig. 3. By comparing the results presented in Figs. 1 and 3, it can be seen that the presence of water in the reaction stream only slightly affected the activity of the catalyst at temperatures lower than 250°C. On the other hand, an enhanced catalytic activity at temperatures above 250°C is obtained. In particular, at 400°C the NO conversion increases remarkably from 15 to 45% in the presence of water. The  $N_2$  selectivity is also significantly affected by the presence of water in the feed stream. A  $N_2$  selectivity value of 87% is now obtained at the temperature of maxi-

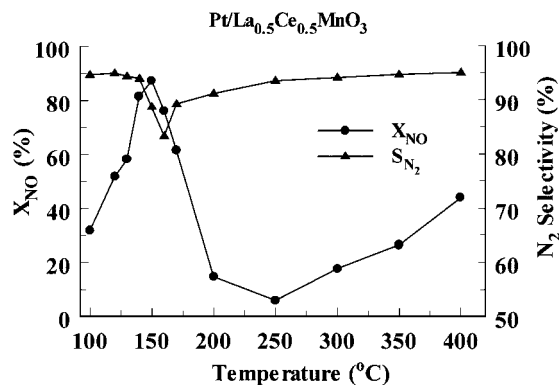


FIG. 3. Effect of 5%  $H_2O$  in the feed stream on NO conversion ( $\bullet$ ) and  $N_2$  selectivity ( $\blacktriangle$ ) as a function of reaction temperature on the 0.1 wt%  $Pt/La_{0.5}Ce_{0.5}MnO_3$  catalyst. Reaction conditions:  $NO = 0.25\%$ ,  $H_2 = 1.0\%$ ,  $O_2 = 5\%$ ,  $H_2O = 5\%$ ,  $W = 0.15g$ ,  $GHSV = 80,000 h^{-1}$ .

imum NO conversion, while values in the 90–95% range are obtained at  $T > 250^\circ C$ .

Figure 4 presents comparative results of the integral rate per gram of catalyst for  $N_2$  formation (Fig. 4a) and  $N_2O$  formation (Fig. 4b) among the  $Pt/La_{0.5}Ce_{0.5}MnO_3$  and  $Pt/Al_2O_3$  catalysts in the 100–400°C range in the case where  $H_2O$  is present in the feed stream. As shown in

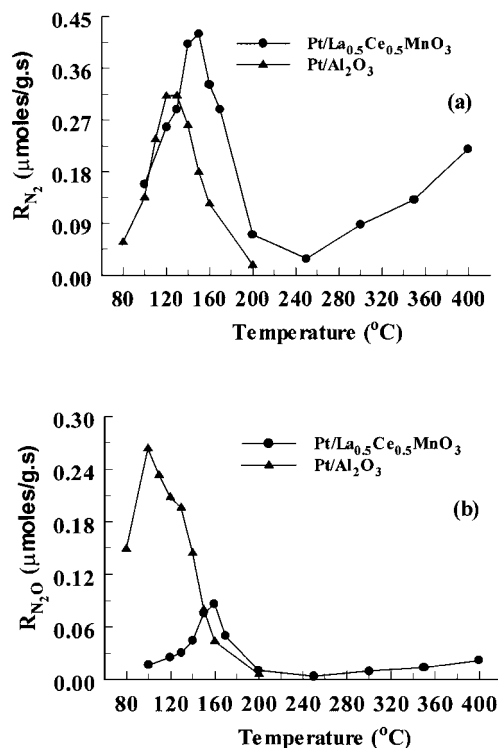


FIG. 4. Effect of 5%  $H_2O$  in the feed stream on (a) integral reaction rate of  $N_2$  and (b)  $N_2O$  formation on the 0.1 wt%  $Pt/La_{0.5}Ce_{0.5}MnO_3$  ( $\bullet$ ) and 0.1 wt%  $Pt/Al_2O_3$  ( $\blacktriangle$ ) catalysts. Reaction conditions:  $H_2 = 1.0\%$ ,  $NO = 0.25\%$ ,  $O_2 = 5\%$ ,  $H_2O = 5\%$ ,  $W = 0.15g$ ,  $GHSV = 80,000 h^{-1}$ .

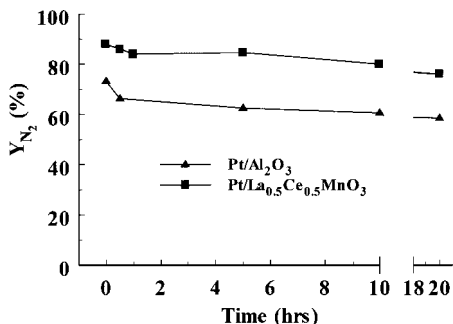


FIG. 5. Stability test on the 0.1 wt% Pt/La<sub>0.5</sub>Ce<sub>0.5</sub>MnO<sub>3</sub> (■) and 0.1 wt% Pt/Al<sub>2</sub>O<sub>3</sub> (▲) catalysts. Reaction conditions: H<sub>2</sub> = 1.0%, NO = 0.25%, O<sub>2</sub> = 5%, H<sub>2</sub>O = 5.0%, W = 0.15 g, GHSV = 80,000 h<sup>-1</sup>.

Fig. 4a, the Pt/La<sub>0.5</sub>Ce<sub>0.5</sub>MnO<sub>3</sub> catalyst exhibits higher rates of N<sub>2</sub> formation than the Pt/Al<sub>2</sub>O<sub>3</sub> catalyst over the whole temperature range of 100–400°C. It is also important to note that at temperatures higher than 250°C the activity of Pt/La<sub>0.5</sub>Ce<sub>0.5</sub>MnO<sub>3</sub> increases with increasing reaction temperature, while there is no activity in the case of Pt/Al<sub>2</sub>O<sub>3</sub> catalyst. In the case of the integral rate of N<sub>2</sub>O formation, the results presented in Fig. 4b are similar to those of Fig. 2b but the differences between the two catalysts are more pronounced. Figure 4b clearly indicates that the Pt/Al<sub>2</sub>O<sub>3</sub> presents much higher rates of N<sub>2</sub>O production than the Pt/La<sub>0.5</sub>Ce<sub>0.5</sub>MnO<sub>3</sub> catalyst in the 100–200°C range. It should be pointed out that the positive effect of the La<sub>0.5</sub>Ce<sub>0.5</sub>MnO<sub>3</sub> support on the activity and N<sub>2</sub> selectivity of supported Pt catalyst is significantly improved by the presence of water.

The stability of the catalyst performance with time on stream was examined on both the Pt/La<sub>0.5</sub>Ce<sub>0.5</sub>MnO<sub>3</sub> and Pt/Al<sub>2</sub>O<sub>3</sub> catalysts under a feed containing 0.25% NO/1.0% H<sub>2</sub>/5% O<sub>2</sub>/5% H<sub>2</sub>O/He. Experiments were conducted for 20 h of continuous reaction. Figure 5 presents results of these experiments in terms of N<sub>2</sub> product yield (Y<sub>N<sub>2</sub></sub>, %). It is observed that for both catalysts the N<sub>2</sub> yield changes only by 5 percentage units during the first 10 h of reaction. In the case of Pt/Al<sub>2</sub>O<sub>3</sub>, the N<sub>2</sub> yield remains the same during the next 10 h on stream but in the case of Pt/La<sub>0.5</sub>Ce<sub>0.5</sub>MnO<sub>3</sub> it drops by 6 percentage units. For the latter catalyst, there is about a 12% drop of its initial N<sub>2</sub> yield after 20 h on stream. It is noted that after 20 h on stream the Pt/La<sub>0.5</sub>Ce<sub>0.5</sub>MnO<sub>3</sub> still exhibits a value of N<sub>2</sub> yield higher by almost 20 percentage units than that of the Pt/Al<sub>2</sub>O<sub>3</sub> catalyst (Fig. 5).

### 3.3. Catalysts Performance for the NO/H<sub>2</sub> Reaction

The catalytic activity of Pt/La<sub>0.5</sub>Ce<sub>0.5</sub>MnO<sub>3</sub> and Pt/Al<sub>2</sub>O<sub>3</sub> solids was also tested in the absence of oxygen using a feed composition of 0.25% NO/1.0% H<sub>2</sub>/He. Figure 6 presents results of the NO conversion (Fig. 6a) and N<sub>2</sub> selectivity (Fig. 6b) obtained on both catalysts in the 100–400°C range. As shown in Fig. 6a, the NO conversion increases signifi-

cantly in the 100–150°C range, while a smaller increase is observed in the 200–400°C range over both catalysts. A 95% conversion of NO is achieved at 400°C in the case of Pt/La<sub>0.5</sub>Ce<sub>0.5</sub>MnO<sub>3</sub> catalyst. It is clearly seen in Fig. 6a that the Pt/La<sub>0.5</sub>Ce<sub>0.5</sub>MnO<sub>3</sub> exhibits significantly higher NO conversion values than the Pt/Al<sub>2</sub>O<sub>3</sub> catalyst in the 150–400°C range. A similar behavior is obtained for the N<sub>2</sub> selectivity of the NO/H<sub>2</sub> reaction but at lower temperatures (100–200°C, Fig. 6b). N<sub>2</sub> selectivity values in the 55–95% range are obtained for temperatures in the 100–400°C range. At 100°C, a TOF value of 10.6 × 10<sup>-3</sup> s<sup>-1</sup> is obtained on both catalysts. It is noted that the temperature profile of X<sub>NO</sub> for the NO/H<sub>2</sub> reaction in the 100–400°C range is completely different than that obtained for the NO/H<sub>2</sub>/O<sub>2</sub> reaction (Fig. 1).

### 3.4. Kinetic Rates and Activation Energies of the NO/H<sub>2</sub>/O<sub>2</sub>, NO/O<sub>2</sub>, and H<sub>2</sub>/O<sub>2</sub> Reactions

Kinetic aspects of the reduction of NO by H<sub>2</sub> in the presence of O<sub>2</sub> have been studied by measurements of the intrinsic rates of the NO/H<sub>2</sub>/O<sub>2</sub>, NO/O<sub>2</sub>, and H<sub>2</sub>/O<sub>2</sub> reactions at 140°C. In addition, the apparent activation energy of the NO/H<sub>2</sub>/O<sub>2</sub> reaction for both catalyst formulations has been estimated. The rate results obtained are given in Table 4 in

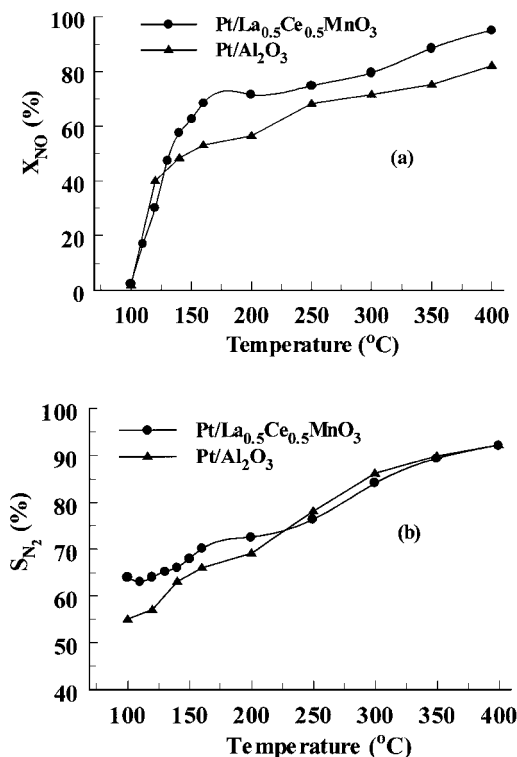


FIG. 6. Temperature profiles of (a) the NO conversion and (b) the N<sub>2</sub> selectivity for the NO/H<sub>2</sub> reaction on the 0.1 wt% Pt/La<sub>0.5</sub>Ce<sub>0.5</sub>MnO<sub>3</sub> (●) and 0.1 wt% Pt/Al<sub>2</sub>O<sub>3</sub> (▲) catalysts. Reaction conditions: H<sub>2</sub> = 1.0%, NO = 0.25%, W = 0.15 g, GHSV = 80,000 h<sup>-1</sup>.

**TABLE 4**  
**Intrinsic Reaction Rates of NO/H<sub>2</sub>/O<sub>2</sub>, NO/O<sub>2</sub>, and H<sub>2</sub>/O<sub>2</sub>**  
**Reactions on Supported Pt Catalysts at T = 140°C**

Catalyst	Reaction	Rate ( $\mu\text{mol/g}\cdot\text{s}$ )	TOF( $\text{s}^{-1}$ )
0.1 wt% Pt/Al <sub>2</sub> O <sub>3</sub>	0.25% NO/1.0% H <sub>2</sub> /5.0% O <sub>2</sub>	1.22 <sup>a</sup>	0.265
0.1 wt% Pt/ La <sub>0.5</sub> Ce <sub>0.5</sub> MnO <sub>3</sub>		2.26 <sup>a</sup>	0.490
0.1 wt% Pt/Al <sub>2</sub> O <sub>3</sub>	0.25% NO/5.0% O <sub>2</sub>	0.017 <sup>a</sup>	0.0037
0.1 wt% Pt/ La <sub>0.5</sub> Ce <sub>0.5</sub> MnO <sub>3</sub>		0.043 <sup>a</sup>	0.0093
0.1 wt% Pt/Al <sub>2</sub> O <sub>3</sub>	1.0% H <sub>2</sub> /5.0% O <sub>2</sub>	62.7 <sup>b</sup>	13.6
0.1 wt% Pt/ La <sub>0.5</sub> Ce <sub>0.5</sub> MnO <sub>3</sub>		51.2 <sup>b</sup>	11.1

<sup>a</sup> Micromoles of NO per gram per second.

<sup>b</sup> Micromoles of H<sub>2</sub> per gram per second.

terms of micromoles per gram per second and TOF ( $\text{s}^{-1}$ ) along with the feed composition used for each reaction. In the case of NO/O<sub>2</sub> reaction, only NO<sub>2</sub> was observed with a rate value 2 orders of magnitude smaller than that observed for the desired NO/H<sub>2</sub>/O<sub>2</sub> reaction. On the other hand, in the case of H<sub>2</sub> combustion (1% H<sub>2</sub>/5% O<sub>2</sub>/He) the observed rate is now 50 times higher than that of the desired NO/H<sub>2</sub>/O<sub>2</sub> reaction in the case of Pt/Al<sub>2</sub>O<sub>3</sub> and 22.5 times higher in the case of Pt/La<sub>0.5</sub>Ce<sub>0.5</sub>MnO<sub>3</sub> catalyst. The significance of these results will be discussed later. It is worth mentioning here that a spillover mechanism of H<sub>2</sub> was observed during H<sub>2</sub>/O<sub>2</sub>/He reaction on the basis of monitoring H<sub>2</sub> consumption. In particular, in the case of Pt/Al<sub>2</sub>O<sub>3</sub> catalyst the H<sub>2</sub> conversion as a function of time on stream was as follows:  $X_{\text{H}_2}$  (%) = 100, 100, 80, 55, 32, 20.5, and 20.2 after 0.1, 30, 60, 90, 120, 180, and 300 min, respectively. Thus, a true steady state rate for H<sub>2</sub> combustion was achieved after 3 h on stream (5 mg of Pt/Al<sub>2</sub>O<sub>3</sub> diluted in 45 mg of Al<sub>2</sub>O<sub>3</sub>,

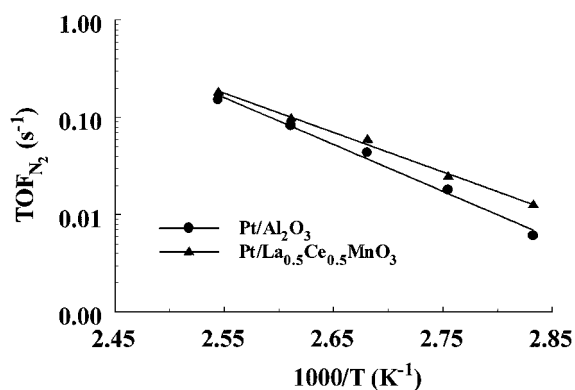


**FIG. 7.** Arrhenius plots of the rate (TOF,  $\text{s}^{-1}$ ) of N<sub>2</sub> formation of the NO/H<sub>2</sub>/O<sub>2</sub> lean de-NO<sub>x</sub> reaction on the 0.1 wt% Pt/La<sub>0.5</sub>Ce<sub>0.5</sub>MnO<sub>3</sub> (▲) and 0.1 wt% Pt/Al<sub>2</sub>O<sub>3</sub> (●) catalysts. Feed composition: H<sub>2</sub> = 1.0%, NO = 0.25%, O<sub>2</sub> = 5%, He as balance gas.

$Q = 200 \text{ cm}^3/\text{min}$ ). In the case of the Pt/La<sub>0.5</sub>Ce<sub>0.5</sub>MnO<sub>3</sub> catalyst, after 2 h on stream a steady state conversion of hydrogen ( $X_{\text{H}_2} = 16.5\%$ ) was achieved. It is noted that no hydrogen combustion activity was observed for the supports alone under the same reaction conditions.

Figure 7 shows Arrhenius plots for the estimation of the apparent activation energy of the NO/H<sub>2</sub>/O<sub>2</sub> reaction. Measurements were taken in the 90–130°C range with a feed consisting of 0.25% NO/1% H<sub>2</sub>/5% O<sub>2</sub>/He. Apparent activation energy values of 21.5 and 24.8 kcal/mol were calculated for the Pt/La<sub>0.5</sub>Ce<sub>0.5</sub>MnO<sub>3</sub> and Pt/Al<sub>2</sub>O<sub>3</sub> catalysts, respectively. These results are in harmony with the higher reaction rates observed on the former than the latter catalyst formulation (see Fig. 2).

### 3.5. Surface Reactivity Studies by Transient Methods

**3.5.1. NO TPDs.** The chemical interaction of NO with the surface of La<sub>0.5</sub>Ce<sub>0.5</sub>MnO<sub>3</sub> and Al<sub>2</sub>O<sub>3</sub> supports as well as of the 0.1 wt% Pt/La<sub>0.5</sub>Ce<sub>0.5</sub>MnO<sub>3</sub> and 0.1 wt% Pt/Al<sub>2</sub>O<sub>3</sub>-supported catalysts was studied by adsorption experiments of NO at room temperature followed by temperature-programmed desorption (TPD) in He flow. Before NO chemisorption took place the La<sub>0.5</sub>Ce<sub>0.5</sub>MnO<sub>3</sub> and Al<sub>2</sub>O<sub>3</sub> samples were pretreated with air (30 cm<sup>3</sup> (STP)/min) at 650°C for 2 h, while the supported Pt catalyst samples were pretreated in air at 400°C for 2 h followed by H<sub>2</sub> treatment at 300°C for 2 h.

Figure 8 shows TPD response curves of NO and N<sub>2</sub>O for all the studied materials. In the case of La<sub>0.5</sub>Ce<sub>0.5</sub>MnO<sub>3</sub> solid (Fig. 8a), one distinct NO desorption peak is obtained at  $T_M = 365^\circ\text{C}$  with a shoulder at the rising part of it. A broad N<sub>2</sub>O peak is obtained at  $T_M = 620^\circ\text{C}$ , while a very small peak at  $T_M = 280^\circ\text{C}$  is also observed. However, in the case of 0.1 wt% Pt/La<sub>0.5</sub>Ce<sub>0.5</sub>MnO<sub>3</sub> catalyst (Fig. 8b) two distinct NO desorption peaks with peak maxima at low temperatures are observed. The first peak (the numbering of desorption peaks follows the direction of increasing temperature) is centered at 65°C, while the second sharper peak is centered at 120°C. A small N<sub>2</sub>O peak appears in the 130–185°C range as opposed to the case of La<sub>0.5</sub>Ce<sub>0.5</sub>MnO<sub>3</sub> support where a much larger N<sub>2</sub>O peak appears at much higher temperatures. The amount of desorbed NO and N<sub>2</sub>O over the two solids is substantially different. The quantities obtained (micromoles per gram) are given in Table 5. In the case of supported Pt catalyst an amount of desorbed NO 2.1 times lower than that obtained on La<sub>0.5</sub>Ce<sub>0.5</sub>MnO<sub>3</sub> support is noted.

In the case of Al<sub>2</sub>O<sub>3</sub> (Fig. 8c), only NO is observed to desorb. Two main desorption peaks are obtained centered at 375°C and 525°C, while a very small peak is observed at 75°C. In the case of 0.1 wt% Pt/Al<sub>2</sub>O<sub>3</sub> catalyst (Fig. 8d), besides NO, nitrous oxide (N<sub>2</sub>O) is observed in the TPD spectrum. A large NO peak is centered at about 240°C and two smaller NO peaks are centered at 420°C and 470°C.

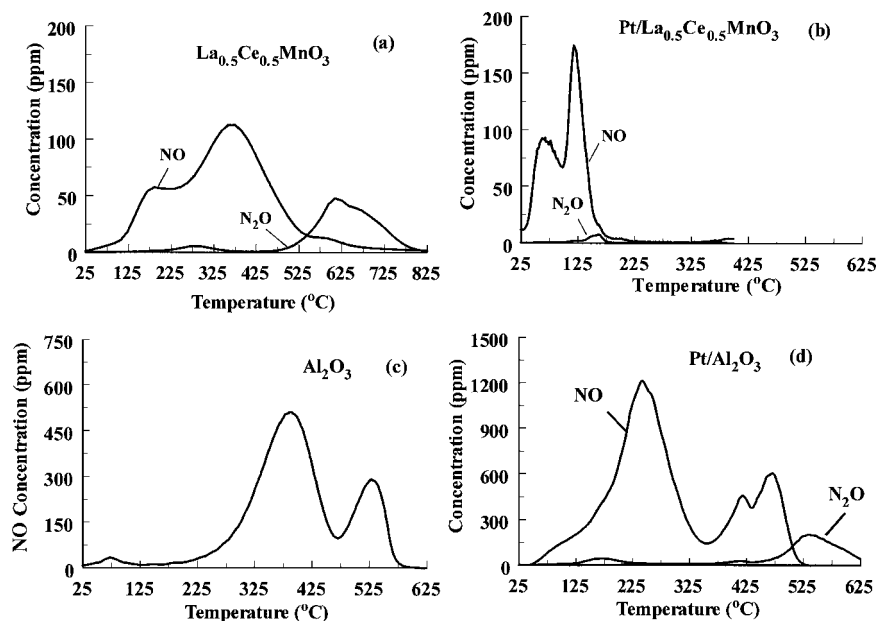


**FIG. 8.** Temperature-programmed desorption (TPD) profiles of NO, N<sub>2</sub>, and N<sub>2</sub>O in He flow according to Experiment A (Table 1) on (a) La<sub>0.5</sub>Ce<sub>0.5</sub>MnO<sub>3</sub> ( $W=0.2$  g), (b) 0.1 wt% Pt/La<sub>0.5</sub>Ce<sub>0.5</sub>MnO<sub>3</sub> ( $W=0.15$  g), (c) Al<sub>2</sub>O<sub>3</sub> ( $W=0.15$  g), and (d) 0.1 wt% Pt/Al<sub>2</sub>O<sub>3</sub> ( $W=0.15$  g);  $\beta = 30^\circ\text{C}/\text{min}$ ,  $Q_{\text{He}} = 30$  cm<sup>3</sup>/min.

A small N<sub>2</sub>O peak is observed at 535°C and a very small one appears in the 120–230°C range. The NO desorption spectrum observed on Pt/Al<sub>2</sub>O<sub>3</sub> shifted to lower temperatures compared to that obtained with the Al<sub>2</sub>O<sub>3</sub> support. By comparing the TPD results obtained on both supported Pt catalysts, two distinct differences must be noted. First, the Pt/Al<sub>2</sub>O<sub>3</sub> desorbs about 5 times more NO than the Pt/La<sub>0.5</sub>Ce<sub>0.5</sub>MnO<sub>3</sub> catalyst (see Table 5, Expt A). Second, practically all the adsorbed NO desorbs at  $T < 200^\circ\text{C}$  in the

case of Pt/La<sub>0.5</sub>Ce<sub>0.5</sub>MnO<sub>3</sub>, while only 10% of NO desorbs at  $T < 200^\circ\text{C}$  in the case of Pt/Al<sub>2</sub>O<sub>3</sub> catalyst. Further discussion on the TPDs of Fig. 8 will be provided in a following section.

**3.5.2. TPSR in He flow following NO/H<sub>2</sub>/O<sub>2</sub> reaction.** The measurement of NO chemisorption under NO/H<sub>2</sub>/O<sub>2</sub> reaction conditions on the 0.1 wt% Pt/La<sub>0.5</sub>Ce<sub>0.5</sub>MnO<sub>3</sub> and 0.1 wt% Pt/Al<sub>2</sub>O<sub>3</sub> catalysts was attempted as follows. After reaction with the 0.25% NO/1.0% H<sub>2</sub>/5% O<sub>2</sub>/He gas mixture at 140°C for 30 min (steady state), the reactor was quickly cooled to room temperature under the reaction mixture. The feed was then changed to He for 5 min to purge the gas phase from reactor and the lines. The temperature of the catalyst was then increased at the rate of 30°C/min to carry out a TPSR experiment. Figures 9a–9d present transient response curves of NO, N<sub>2</sub>O, N<sub>2</sub>, and NO<sub>2</sub> obtained over La<sub>0.5</sub>Ce<sub>0.5</sub>MnO<sub>3</sub>, Pt/La<sub>0.5</sub>Ce<sub>0.5</sub>MnO<sub>3</sub>, Al<sub>2</sub>O<sub>3</sub>, and Pt/Al<sub>2</sub>O<sub>3</sub> catalysts. In the case of La<sub>0.5</sub>Ce<sub>0.5</sub>MnO<sub>3</sub> solid, two NO desorption peaks of about the same peak maximum intensity are obtained. The first peak is centered at 100°C, while the second one is centered at 265°C. In the case of Pt/La<sub>0.5</sub>Ce<sub>0.5</sub>MnO<sub>3</sub>, transient response curves of NO, N<sub>2</sub>O, and N<sub>2</sub> are observed. More precisely, a broad NO peak is observed in the 25–150°C range and a smaller one at 175°C. A very small and broad N<sub>2</sub>O peak is observed in the 100–190°C range, and a N<sub>2</sub> peak at  $T_M = 200^\circ\text{C}$ .

In the case of Al<sub>2</sub>O<sub>3</sub> (Fig. 9c), a very large NO desorption peak centered at 250°C is observed along with a smaller NO<sub>2</sub> peak centered at 625°C. A totally different TPSR spectrum is observed in the case of Pt/Al<sub>2</sub>O<sub>3</sub> (Fig. 9d). Two very

**TABLE 5**

**Amount of Species Desorbed ( $\mu\text{mol}/\text{g}_{\text{cat}}$ ) during Various Kinds of Temperature-Programmed Desorption (TPD) and Surface Reaction (TPSR) Experiments in Different Gas Atmospheres as a Function of Catalyst Composition**

Catalyst sample	Expt (Table 1)	Species					Total N-containing species
		NO	N <sub>2</sub> O	N <sub>2</sub>	NO <sub>2</sub>	NH <sub>3</sub>	
0.1% Pt/La <sub>0.5</sub> Ce <sub>0.5</sub> MnO <sub>3</sub>	A	2.95	0.03				3.01 ( $\theta = 0.65$ )
	B	3.23	0.02	0.47			4.21 ( $\theta = 0.92$ )
	C	3.53	0.28			0.02	4.11 ( $\theta = 0.89$ )
0.1% Pt/Al <sub>2</sub> O <sub>3</sub>	A	14.25	1.6				17.45
	B	13.12	0.81	12.43			39.6
	C			18.83			37.7
La <sub>0.5</sub> Ce <sub>0.5</sub> MnO <sub>3</sub>	A	6.26	0.8				7.86
	B	5.65					5.65
Al <sub>2</sub> O <sub>3</sub>	A	7.31					7.31
	B	25.01			11.02		36.03

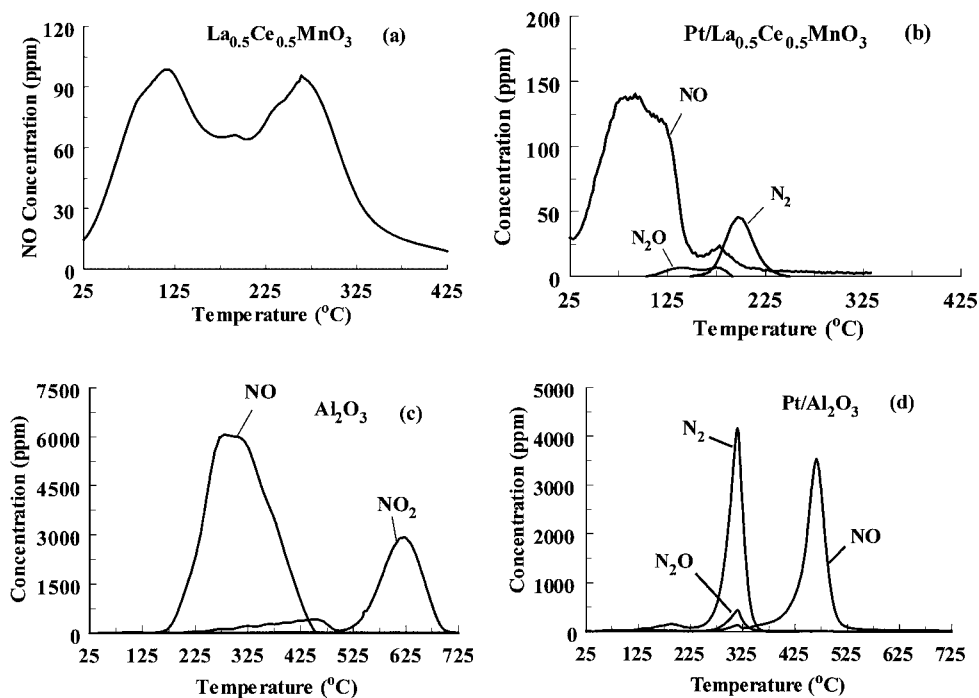


FIG. 9. Transient response curves of NO, N<sub>2</sub>, N<sub>2</sub>O, and NO<sub>2</sub> obtained during TPSR in He flow following reaction in NO/H<sub>2</sub>/O<sub>2</sub> on the (a) La<sub>0.5</sub>Ce<sub>0.5</sub>MnO<sub>3</sub>, (b) 0.1 wt% Pt/La<sub>0.5</sub>Ce<sub>0.5</sub>MnO<sub>3</sub>, (c) Al<sub>2</sub>O<sub>3</sub>, and (d) 0.1 wt% Pt/Al<sub>2</sub>O<sub>3</sub> catalysts;  $Q_{\text{He}} = 30 \text{ cm}^3/\text{min}$ ,  $\beta = 30^\circ\text{C}/\text{min}$ .

large and intense peaks centered at 305°C and 470°C corresponding to N<sub>2</sub> and NO, respectively, are observed. A small N<sub>2</sub>O peak is also seen at 310°C. We note the fact that the amount of NO desorbed from Al<sub>2</sub>O<sub>3</sub> is about twice the amount of N<sub>2</sub> desorbed from Pt/Al<sub>2</sub>O<sub>3</sub>, while the amount of NO<sub>2</sub> desorbed from Al<sub>2</sub>O<sub>3</sub> is similar to that of NO desorbed from Pt/Al<sub>2</sub>O<sub>3</sub>. In addition, the amount of N<sub>2</sub> produced by the latter catalyst is found to be about 26 times larger than the amount observed on Pt/La<sub>0.5</sub>Ce<sub>0.5</sub>MnO<sub>3</sub> catalyst. Table 5 (Expt B) reports the amounts of NO, N<sub>2</sub>O, NO<sub>2</sub>, and N<sub>2</sub> measured by the He TPSR experiments presented in Figs. 9a–9d.

### 3.5.3. TPSR in H<sub>2</sub>/He flow following NO/H<sub>2</sub>/O<sub>2</sub> reaction.

Figure 10 describes TPSR response curves of NO, N<sub>2</sub>O, N<sub>2</sub>, and NH<sub>3</sub> obtained in H<sub>2</sub>/He flow (Expt C, Table 1) on the Pt/La<sub>0.5</sub>Ce<sub>0.5</sub>MnO<sub>3</sub> and Pt/Al<sub>2</sub>O<sub>3</sub> catalysts following reaction in NO/H<sub>2</sub>/O<sub>2</sub> at 140°C and quick cooling of the sample to room temperature in the reaction mixture. In the case of Pt/La<sub>0.5</sub>Ce<sub>0.5</sub>MnO<sub>3</sub> (Fig. 10a), response curves corresponding to NO, N<sub>2</sub>O, and NH<sub>3</sub> are obtained. A desorption peak of NO centered at 40°C with a tail out to 225°C is observed. A very small peak of NH<sub>3</sub> centered at 50°C and a very broad N<sub>2</sub>O peak in the 25–175°C range are also observed. However, in the case of Pt/Al<sub>2</sub>O<sub>3</sub> (Fig. 10b) only a N<sub>2</sub> response curve is obtained with four peaks in the 125–425°C range. The amounts of gaseous species formed in the H<sub>2</sub> TPSR experiments (Fig. 10) are reported in Table 5 (Expt C).

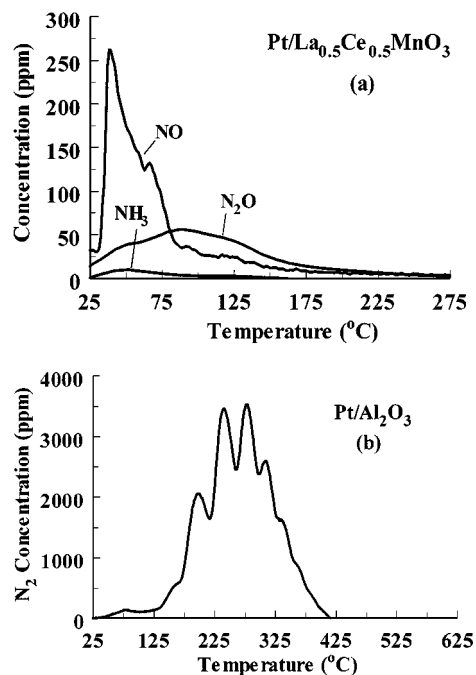


FIG. 10. Transient response curves of NO, NH<sub>3</sub>, N<sub>2</sub>, and N<sub>2</sub>O gaseous species obtained during TPSR in 10% H<sub>2</sub>/He flow on the (a) 0.1 wt% Pt/La<sub>0.5</sub>Ce<sub>0.5</sub>MnO<sub>3</sub> and (b) 0.1 wt% Pt/Al<sub>2</sub>O<sub>3</sub> catalysts according to the sequence of steps described in Experiment C (Table 3);  $Q = 30 \text{ cm}^3/\text{min}$ ,  $\beta = 30^\circ\text{C}/\text{min}$ .

## 4. DISCUSSION

### 4.1. Catalysts Performance

The remarkable catalytic performance of the present 0.1 wt% Pt/La<sub>0.5</sub>Ce<sub>0.5</sub>MnO<sub>3</sub> catalyst toward NO/H<sub>2</sub>/O<sub>2</sub> (lean-deNO<sub>x</sub>) reaction in the 100–200°C low-temperature range and in the presence of 5% H<sub>2</sub>O in the feed stream is best illustrated in Table 6 by comparison with other Pt-based catalysts reported in the open literature. In Table 6,  $T_{\max}$  is the reaction temperature at which maximum NO conversion is observed, while  $\Delta T_1$  and  $\Delta T_2$  are the temperature ranges in which  $X_{\text{NO}}$  appears to be greater than 1/2 or 1/10 of the maximum conversion of NO observed, respectively. The latter parameters could be used to define the quality of the operating temperature window. For example, the larger the value of  $\Delta T_1$  the better the desired operation of the catalyst under practical conditions. Table 6 reports also the integral rate of N<sub>2</sub> production per gram of Pt metal ( $R_{\text{N}_2}$ ) evaluated according to the  $X_{\text{NO}}$  and  $S_{\text{N}_2}$  values reported. In addition, results of the turnover frequency (based on Pt dispersion values reported) of the N<sub>2</sub> production,  $\text{TOF}_{\text{N}_2}$  (s<sup>-1</sup>) at 130 or 140°C ( $X_{\text{NO}}$  is less than 20% at the feed composition reported) are given in Table 6. First, the comparison among the two catalysts presently investigated is rather straightforward. There is about a 40% increase in the maximum integral rate when Pt is supported on La<sub>0.5</sub>Ce<sub>0.5</sub>MnO<sub>3</sub> than  $\gamma$ -Al<sub>2</sub>O<sub>3</sub> solid, while in terms of  $\text{TOF}$  the increase is even larger (e.g., 85%). In addition, the N<sub>2</sub> selectivity value of 88% obtained on Pt/La<sub>0.5</sub>Ce<sub>0.5</sub>MnO<sub>3</sub>, to our knowledge, is the highest value ever reported at the temperature at which maximum activity is observed for the NO/H<sub>2</sub>/O<sub>2</sub> reaction with 5% H<sub>2</sub>O in the feed stream in

the 100–200°C low-temperature range. According to the results of Table 6, the present Pt/La<sub>0.5</sub>Ce<sub>0.5</sub>MnO<sub>3</sub> catalyst appears to be superior in all respects of its performance to all the other catalysts listed. Given the fact that the reaction orders with respect to all three reactants may not be expected to have values greater than unity, from the results of Table 6 it is clear that the Pt/La<sub>0.5</sub>Ce<sub>0.5</sub>MnO<sub>3</sub> exhibits the highest activity and selectivity ever reported for the NO/H<sub>2</sub>/O<sub>2</sub> reaction.

On the basis of the fact that the present supported Pt catalysts exhibit similar dispersions (~90%), a purely support effect must be invoked to explain the differences in the catalytic performances of these catalyst formulations. It is suggested that one of the main reasons that the Pt/La<sub>0.5</sub>Ce<sub>0.5</sub>MnO<sub>3</sub> catalyst exhibits remarkable N<sub>2</sub> selectivity values compared to Pt/Al<sub>2</sub>O<sub>3</sub> may be the ability of La<sub>0.5</sub>Ce<sub>0.5</sub>MnO<sub>3</sub> support to act as an oxygen reservoir. The latter material consists of CeO<sub>2</sub>, MnO<sub>2</sub>, and LaMnO<sub>3</sub> (of perovskite structure) phases within the pores in which Pt was highly dispersed. These phases contain inherently oxygen vacancies according to O<sub>2</sub> chemisorption experiments performed. More precisely, following O<sub>2</sub> adsorption at 30°C for 0.5 h a TPD run was performed. A large and broad O<sub>2</sub> desorption peak starting at 600°C was obtained that amounted to 32.5  $\mu\text{atom of O/g}_{\text{cat}}$ . This value is about 7 times larger than the amount of exposed Pt atoms in the present supported catalysts. A recent detailed kinetic study of the NO/H<sub>2</sub>/O<sub>2</sub> reaction on Pt–Mo–Co/ $\alpha$ -Al<sub>2</sub>O<sub>3</sub> (17) revealed that for O<sub>2</sub> feed concentrations below 2% the rates of NO conversion and N<sub>2</sub> selectivity both increase significantly with increasing O<sub>2</sub> feed concentration, while co-adsorbed hydrogen was found to displace molecularly adsorbed NO. The authors have suggested that the oxygen promoting

TABLE 6

Catalytic Activity of Various Supported Pt Catalysts for the NO/H<sub>2</sub>/O<sub>2</sub> Reaction in the Low-Temperature Range of 90–200°C

Catalyst	Reaction conditions					$R_{\text{N}_2}$ ( $\mu\text{mol/s.g}_{\text{m}}$ )	$\Delta T_1$ (°C) <sup>a</sup>	$\Delta T_2$ (°C) <sup>b</sup>	$X_{\text{NO}}$ (%)	$S_{\text{N}_2}$ (%)	$\text{TOF}_{\text{N}_2} \times 10^2$ (s <sup>-1</sup> )	Ref.
	NO (%)	H <sub>2</sub> (%)	O <sub>2</sub> (%)	GHSV (h <sup>-1</sup> )	$T_{\max}$ (°C)							
1% Pt/SiO <sub>2</sub>	0.05	0.2	6	240,000	90	7.6	25	60	75	30	1.63 <sup>f</sup>	(18)
1% Pt/Al <sub>2</sub> O <sub>3</sub>	0.05	0.2	6	240,000	140	10.1	40	90	50	60	0.87 <sup>g</sup>	(18)
1% Pt/TiO <sub>2</sub>	0.1	0.3	5.0 <sup>c</sup>	40,000	100	2.2	50	100	50	21	0.17 <sup>f</sup>	(19)
1% Pt/Al <sub>2</sub> O <sub>3</sub>	0.1	0.3	5.0 <sup>c</sup>	40,000	100	1.4	65	120	62.2	11	0.22 <sup>f</sup>	(19)
1% Pt–Mo–Co/Al <sub>2</sub> O <sub>3</sub>	0.3	0.8	8.0	6500	150	12.1	30	70	55	50	0.31 <sup>g</sup>	(17)
0.1% Pt/Al <sub>2</sub> O <sub>3</sub>	0.25	1.0	5.0 <sup>d</sup>	80,000	125	285.8	45	100	66	60	26.5 <sup>f</sup>	This work
0.1% Pt/ La <sub>0.5</sub> Ce <sub>0.5</sub> MnO <sub>3</sub>	0.25	1.0	5.0 <sup>d</sup>	80,000	140	396.9	60	300 <sup>e</sup>	88	79	49.0 <sup>f</sup>	This work

<sup>a</sup>  $\Delta T_1$ : temperature range where  $X_{\text{NO}} > X_{\text{NOmax}}/2$ .

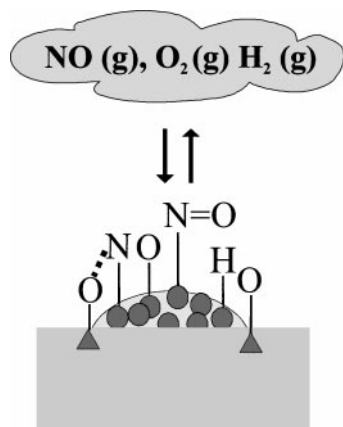
<sup>b</sup>  $\Delta T_2$ : temperature range where  $X_{\text{NO}} > X_{\text{NOmax}}/10$ .

<sup>c</sup> 10% H<sub>2</sub>O is also present in the feed stream.

<sup>d</sup> 10% H<sub>2</sub>O is also present in the feed stream.

<sup>e</sup> Except at  $T = 250^\circ\text{C}$ .

<sup>f</sup>  $T = 140^\circ\text{C}$ . <sup>g</sup>  $T = 130^\circ\text{C}$ .



**SCHEME 1.** Interaction of gaseous NO, O<sub>2</sub>, and H<sub>2</sub> with the 0.1 wt% Pt/La<sub>0.5</sub>Ce<sub>0.5</sub>MnO<sub>3</sub> catalyst.

effect is attributed to the lowering of abundant adsorbed hydrogen atoms by reaction with oxygen to form H<sub>2</sub>O, permitting therefore the pairing of two adjacent adsorbed N atoms to form N<sub>2</sub> gas. This explanation might also be offered to explain the N<sub>2</sub> selectivity behavior of the present supported Pt catalysts. In fact, higher N<sub>2</sub> selectivity values are obtained in the 100–200°C range in the presence than the absence of O<sub>2</sub> in the feed stream (see Figs. 2a and 6a). It is suggested that the rate of removal of adsorbed hydrogen atoms on the small Pt particles might be enhanced by the participation of oxygen atoms present at the interface between the Pt particles and support. Such oxygen atoms could be more active than oxygen atoms on the Pt surface toward reaction with adsorbed hydrogen. Scheme 1 shows the formation of adsorbed oxygen species on the Pt metal and La<sub>0.5</sub>Ce<sub>0.5</sub>MnO<sub>3</sub> support. For the latter, anionic vacant sites present in LaMnO<sub>3</sub>, CeO<sub>2</sub>, and MnO<sub>2</sub> but not in  $\gamma$ -Al<sub>2</sub>O<sub>3</sub> support phases are offered for O<sub>2</sub> chemisorption (16, 24, 25).

The adjustment of reaction N<sub>2</sub> selectivity by the catalyst is an aspect the understanding of which requires precise information about the catalytic mechanism and intrinsic kinetics of the reaction. This matter was out of the scope of the present work. However, some remarks based on the present results could be made. On supported Rh catalysts the formation of Rh–NO<sup>–</sup> species is well documented (26–28). Dissociation of the latter species is expected to occur easier than of other chemisorbed NO species (e.g., Rh–NO (neutral) and Rh–NO<sup>+</sup>). The presence of F-type defects in the La<sub>0.5</sub>Ce<sub>0.5</sub>MnO<sub>3</sub> support as previously discussed and the fact that NO can be adsorbed onto these sites (29) make possible the likelihood of formation of negatively charged adsorbed NO species at the metal–support interface as illustrated in Scheme 1. In this chemisorbed state the N atom is bonded to the Pt metal and the O atom is bonded to the oxygen vacancy. This possibility is not offered in the case of Pt/Al<sub>2</sub>O<sub>3</sub>. Therefore, the rate of dissociation of NO on Pt/La<sub>0.5</sub>Ce<sub>0.5</sub>MnO<sub>3</sub> is expected to be larger than that occur-

ring on Pt/Al<sub>2</sub>O<sub>3</sub>, if the surface coverage of NO does not much influence this rate. *In situ* FTIR studies provide the means to probe in a direct manner for the presence of such an adsorbed NO structure. This kind of investigation will be conducted and results will soon be reported.

It has been shown (24) that after passing NO/O<sub>2</sub> gas mixture over the MnO<sub>y</sub>–ZrO<sub>2</sub> system the MnO<sub>y</sub> phase acts as a reservoir of lattice oxygen (due to its oxygen vacant sites) that can oxidize NO to NO<sub>2</sub>. The latter species is then transferred and stored on the ZrO<sub>2</sub> surface. It has also been suggested that on the Pt/Al<sub>2</sub>O<sub>3</sub> catalyst reduction of NO by C<sub>3</sub>H<sub>6</sub> to produce N<sub>2</sub> gas in the presence of 5% O<sub>2</sub> proceeds via an NO<sub>2</sub>-adsorbed intermediate species that is more active than the adsorbed NO species (30). The results in Table 4, aiming to shed some light on the role of NO<sub>2</sub> on the activity behavior of the present supported Pt catalysts, need to be interpreted with care. If one assumes that the NO<sub>2</sub> is an important intermediate species in the sequence of steps for the formation of N<sub>2</sub> gas during the NO/H<sub>2</sub>/O<sub>2</sub>/He reaction, the measured steady state production rates of NO<sub>2</sub> during the NO/O<sub>2</sub>/He reaction cannot directly be associated with the former rate. The low value of the steady state rate of NO<sub>2</sub> formation reported in Table 4 does not imply the absence of a reservoir of adsorbed NO<sub>2</sub> on the metal and/or support that might be more active than the molecularly adsorbed NO under lean-NO<sub>x</sub> conditions. The He TPSR experiments reported in Fig. 9 and Table 5 suggest the formation of a large amount of NO<sub>2</sub> on the alumina surface but the Pt/Al<sub>2</sub>O<sub>3</sub> appears less active and selective than the Pt/La<sub>0.5</sub>Ce<sub>0.5</sub>MnO<sub>3</sub> catalyst.

Two maxima in the temperature profile of NO conversion ( $T_{\max} = 100$  and 300°C) for the NO/H<sub>2</sub>/O<sub>2</sub> reaction have been reported on Pd/TiO<sub>2</sub> catalyst (19). The authors have suggested that the cause of the appearance of the two maxima is the change of the reaction paths between the direct reduction of NO by H<sub>2</sub> and the reduction of *in situ* generated NO<sub>2</sub> by H<sub>2</sub>. According to the catalytic results of the present Pt/La<sub>0.5</sub>Ce<sub>0.5</sub>MnO<sub>3</sub> and La<sub>0.5</sub>Ce<sub>0.5</sub>MnO<sub>3</sub> solids, the appearance of two maxima in the activity vs temperature profile in the 100–500°C range is due to the bifunctional operation of the catalyst. The Pt metal operates in the 100–200°C range, while the La<sub>0.5</sub>Ce<sub>0.5</sub>MnO<sub>3</sub> support in the 250–500°C range where the operation of the latter is influenced by the Pt metal.

A maximum in the activity vs temperature profile observed at 140°C (Figs. 1a and 2a) is rather clear that is due to the significant rate of H<sub>2</sub> combustion to H<sub>2</sub>O on the Pt surface in the 100–250°C range according to the kinetic rates reported in Table 4. Other researchers (17, 19) have also suggested this explanation. In particular, Ueda *et al.* (19) have measured on the 1 wt% Pt/Al<sub>2</sub>O<sub>3</sub> catalyst the rate of H<sub>2</sub> combustion at 300°C. The latter rate was 30 times larger than that obtained for the NO/H<sub>2</sub> reaction.

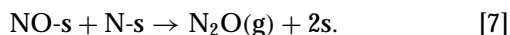
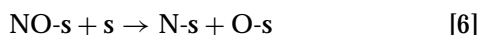
Hodjati *et al.* (31) and Eguchi *et al.* (32) have reported results on the beneficial effect of H<sub>2</sub>O on the adsorptive

capacity of some perovskites ABO<sub>3</sub> (A = Ca, Sr, Ba and B = Sn, Zr, Ti) and Mn–Zr mixed oxides, respectively, toward NO and NO<sub>2</sub> under lean-burn conditions. The authors have suggested that adsorbed water stabilizes adsorbed NO<sub>3</sub><sup>-</sup> species through hydration, the latter species formed via NO and NO<sub>2</sub> adsorption. A similar explanation might be offered for the significant increase of NO conversion in the 300–400°C range (Fig. 3) that takes place mainly on the La<sub>0.5</sub>Ce<sub>0.5</sub>MnO<sub>3</sub> support. On the other hand, the less pronounced beneficial effect of water observed in the 100–200°C range (Figs. 3 and 4) could be explained on the basis of the role of adsorbed hydrogen (produced by H<sub>2</sub>O dissociation on the Pt metal) to regulate the surface atomic composition of H<sub>s</sub> and O<sub>s</sub>. The rate of water dissociation under the reaction conditions may be small enough to significantly affect the NO conversion and N<sub>2</sub> reaction selectivity.

#### 4.2. Transient Studies

**4.2.1. NO TPDs.** By comparing the TPD spectra shown in Figs. 8a–8d and the quantities of each species desorbed (Expt A, Table 5) from the supported Pt catalysts and their supports alone, the following are noted.

**Pt/La<sub>0.5</sub>Ce<sub>0.5</sub>MnO<sub>3</sub> catalyst.** In the case of Pt/La<sub>0.5</sub>Ce<sub>0.5</sub>MnO<sub>3</sub> and its support alone, it is found that the latter adsorbs higher amounts of NO than the supported Pt catalyst. Furthermore, the desorption spectra (shape and position) are quite different among the two samples. It is suggested that the small Pt clusters deposited on the La<sub>0.5</sub>Ce<sub>0.5</sub>MnO<sub>3</sub> support have considerably altered the adsorptive characteristics of certain type(s) of its NO chemisorption sites (probably via short-range electronic interactions), while at the same time they may have blocked adsorption sites to a given extent. It is known that chemisorption of NO on metal oxides proceeds with the participation of metal cations, oxygen anions, and oxygen vacant sites forming various kinds of nitrate and nitrite structures (33). From Figs. 8a and 8b it can be stated that breaking of the N–O bond proceeds with much more difficulty on the La<sub>0.5</sub>Ce<sub>0.5</sub>MnO<sub>3</sub> support alone than on the supported Pt metal in order to form N<sub>2</sub>O gas. The following widely accepted elementary steps describe the formation of N<sub>2</sub>O on the Pt surface.



Two clear adsorbed states of NO are formed on the Pt clusters as indicated in Fig. 8b. A NO TPD spectrum very similar in shape to that of Fig. 8b has been reported by Burch *et al.* (34) for the 5 wt% Pt/SiO<sub>2</sub> catalyst after adsorption of NO at room temperature. However, on the latter TPD study two N<sub>2</sub> and N<sub>2</sub>O desorption peaks were observed,

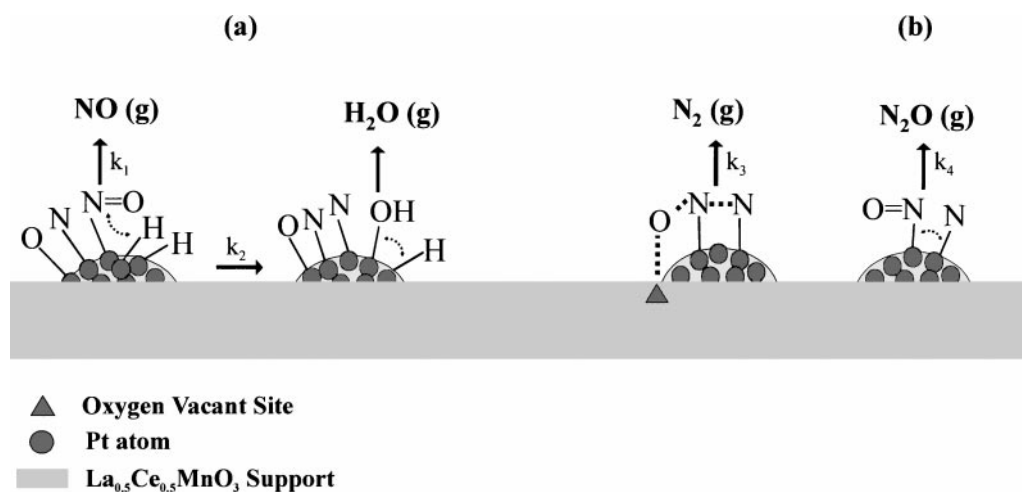
a result quite different than that obtained on the present Pt/La<sub>0.5</sub>Ce<sub>0.5</sub>MnO<sub>3</sub> catalyst. In addition, the *T<sub>M</sub>* value of the second NO peak was found to be significantly higher than that observed on the present Pt/La<sub>0.5</sub>Ce<sub>0.5</sub>MnO<sub>3</sub> system, and about 40% of adsorbed NO participated in the formation of N<sub>2</sub> and N<sub>2</sub>O (34). This result is opposite to that observed here and it shows again the great effect of support on the chemistry of NO adsorption and dissociation over supported Pt catalysts.

**Pt/Al<sub>2</sub>O<sub>3</sub> catalyst.** It is found that the Pt/Al<sub>2</sub>O<sub>3</sub> catalyst adsorbs a much higher amount of NO than that corresponding to the Pt surface and alumina alone (Table 5). This difference cannot be justified even in the case of formation of dinitrosyl (Pt–(NO)<sub>2</sub>) species only. A reasonable mechanism by which the above-mentioned results can be explained is that of NO spillover from the Pt metal to the Al<sub>2</sub>O<sub>3</sub>. By comparing the NO response curves in Figs. 8c and 8d, it can be stated that the large NO desorption peak centered at 240°C represents a new adsorbed state of NO formed by the spillover mechanism.

The formation of N<sub>2</sub>O on the Pt/Al<sub>2</sub>O<sub>3</sub> catalyst in the 425–625°C range is derived via the dissociation of NO onto the Pt metal after desorption of NO from the Al<sub>2</sub>O<sub>3</sub> support. The appearance of the same peak maximum temperature (*T<sub>M</sub>* = 525°C) in the NO response of Al<sub>2</sub>O<sub>3</sub> (Fig. 8c) and that of N<sub>2</sub>O of Pt/Al<sub>2</sub>O<sub>3</sub> (Fig. 8d) strongly supports this view. Even though a spillover mechanism of NO from supported Pt catalysts has not been reported previously to our knowledge, this mechanism was reported to operate in the case of the SCR reaction of NO on the V<sub>2</sub>O<sub>5</sub>/TiO<sub>2</sub> catalyst (35). An alternative explanation for the NO TPD results observed for the Pt/Al<sub>2</sub>O<sub>3</sub> catalyst could be based on the fact that additional sites for NO chemisorption, besides those on Pt and alumina surfaces alone, may have been formed at the periphery of metal–support interaction. However, considering the fact that after subtracting the sum of the amount of NO chemisorption corresponding to the alumina and Pt surface (4.6 μmol/g) alone from the total amount of NO chemisorption, the remaining amount of NO exceeds that which would correspond to adsorption on the Pt surface. This result rather supports the view that the enhanced chemisorption of NO on the Pt/Al<sub>2</sub>O<sub>3</sub> catalyst is at least partly due to a spillover mechanism. The N<sub>2</sub>O produced in the Pt/Al<sub>2</sub>O<sub>3</sub> catalyst in the 425–625°C range (Fig. 8d) is due to reaction of readsorbed NO (after being desorbed from the alumina) with N atoms on Pt according to the elementary reaction steps [5]–[7].

**4.2.2. TPSR experiments in He and H<sub>2</sub> flow following NO/H<sub>2</sub>/O<sub>2</sub> reaction.** The experiments presented in Figs. 9 and 10 reveal important kinetic and mechanistic information for the present catalytic reaction when compared to the ordinary NO TPDs presented in Fig. 8.

**Pt/La<sub>0.5</sub>Ce<sub>0.5</sub>MnO<sub>3</sub> catalyst.** First, the total amount of equivalent N atoms stored on the catalyst surface under

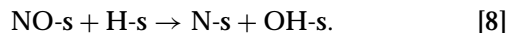


**SCHEME 2.** (a) H-assisted NO desorption and dissociation mechanism and (b) N-assisted reduction mechanism of NO to N<sub>2</sub> and N<sub>2</sub>O on the 0.1 wt% Pt/La<sub>0.5</sub>Ce<sub>0.5</sub>MnO<sub>3</sub> catalyst.

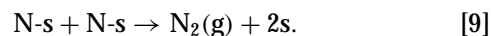
reaction conditions and measured under He (Fig. 9b) and H<sub>2</sub> flow (Fig. 10a) in the TPSR experiments are in excellent agreement (see Table 5, last column). This result confirms the reproducibility and accuracy of the experiments performed. Second, the differences in the spectra shown in Figs. 9b and 10a concern the composition and amounts of gases evolved and therefore reflect the different kinetics of reactions involved under He or H<sub>2</sub> flow. Third, the spectrum of desorbed NO in the H<sub>2</sub> TPSR experiment (Fig. 10a) shifts significantly to lower temperatures compared to the case of He TPD (Fig. 8b) and TPSR (Fig. 9b) experiment. Based on the above-mentioned remarks and the fact that two distinct NO adsorbed states (types I and II) are very likely to have been formed on this catalyst (see Figs. 8b and 9b), the following discussion explains the results of Figs. 9b and 10a in a satisfactory manner.

Scheme 2a illustrates that under NO/H<sub>2</sub>/O<sub>2</sub> reaction conditions adsorbed atomic N, O, and H species can be populated on the catalyst surface in addition to molecularly adsorbed NO. The surface coverage of the adsorbed NO species and its binding energy will depend on the oxidation state of Pt. An assisted hydrogen effect on the lowering of bond strength of Pt–NO might be expected as it has been reported for supported Rh catalysts (36). In the H<sub>2</sub> TPSR experiment, the coverage of adsorbed atomic hydrogen species is expected to be much higher than that found under NO/H<sub>2</sub>/O<sub>2</sub> reaction conditions, while under NO/He adsorption conditions this species cannot be present. Therefore, the shift of desorbed NO response to lower temperatures in the He TPSR (Fig. 9b) and H<sub>2</sub> TPSR (Fig. 10a) experiments with respect to the ordinary NO TPD response (Fig. 8b) can be justified. In Scheme 2a a hydrogen-assisted NO dissociation mechanism, first suggested by Hecker and Bell (8) on the Rh/SiO<sub>2</sub> catalyst, is also proposed. It was

reported (37) that the activation energy of the N–O bond dissociation step [6] is higher than that of the H-assisted N–O bond dissociation step [8] given below.



In Scheme 2b a nitrogen-assisted NO reduction to N<sub>2</sub> and N<sub>2</sub>O is illustrated according to the literature (8, 37). It has been shown that formation of N<sub>2</sub> and N<sub>2</sub>O via these mechanisms proceeds with a lower activation energy barrier than the recombination reaction step [9] of adsorbed atomic N to form N<sub>2</sub> gas.



In Scheme 2b both kinds of adsorbed NO species shown in Scheme 1 could participate in this mechanism. In the ordinary NO TPD (Fig. 8b) it is clearly shown that very little NO dissociation occurs (12% of adsorbed NO, Table 5) that favors the formation of N<sub>2</sub>O. On the other hand, in the case of the He TPSR experiment some coverage of adsorbed atomic N is suggested to be present at the start of the experiment. This species had been formed during NO/H<sub>2</sub>/O<sub>2</sub> reaction. According to Scheme 2b, the rate of nitrogen-assisted NO dissociation becomes significant even at low temperatures and competes favorably with the rate of NO desorption. Given the fact that desorption of NO can now occur at lower temperatures compared to the case of NO TPD (Fig. 8b), the possibility of N<sub>2</sub>O formation now decreases ( $k_1 > k_4$  in Scheme 2), while N<sub>2</sub> can be formed at higher temperatures ( $k_3 < k_4$  in Scheme 2).

In the case of H<sub>2</sub> TPSR experiment (Fig. 10a) it is seen that the formation of N<sub>2</sub>O dominates that of N<sub>2</sub>, while N<sub>2</sub>O is formed in the same temperature range as desorption of

NO occurs. This behavior can be understood on the basis of Scheme 2 where the presence of H<sub>2</sub> gas (10% H<sub>2</sub>/He) promotes significantly the insertion mechanism of N atom to the Pt–NO bond to form N<sub>2</sub>O gas. Thus, when adsorbed N species are present at the start of the H<sub>2</sub> TPSR experiment, the rate of N<sub>2</sub>O formation competes favorably with that of NO desorption, while it is higher than that of N<sub>2</sub> formation ( $k_3 < k_4$  according to the mechanisms of Scheme 2).

According to the He TPSR results reported in Table 5, the NO TPDs of Fig. 8b, and Scheme 2, an upper value for the coverage of adsorbed NO present in the NO/H<sub>2</sub>/O<sub>2</sub> reaction can be suggested for the Pt/La<sub>0.5</sub>Ce<sub>0.5</sub>MnO<sub>3</sub> catalyst. This value is  $\theta_{\text{NO}} < 0.75$ . Much smaller amounts of NH<sub>x</sub> ( $x=0-2$ ) seem to be formed, while the coverage of O and H atoms on Pt seems to be less than about 0.1. These results strongly suggest that dissociation of NO must be considered as a slow step.

*Pt/Al<sub>2</sub>O<sub>3</sub> catalyst.* In the H<sub>2</sub> TPSR experiment (Fig. 10b), only N<sub>2</sub> gas is formed, a result largely different than that obtained on the Pt/La<sub>0.5</sub>Ce<sub>0.5</sub>MnO<sub>3</sub> catalyst (Fig. 10a), while the latter catalyst is found to exhibit significantly higher N<sub>2</sub> selectivity values during the NO/H<sub>2</sub>/O<sub>2</sub> reaction in the 100–200°C range. These two experimental results do not contradict each other. It should be noted that the oxidation state of surface Pt atoms is an important surface parameter that will determine the bond strength among the various adsorbed species and the Pt atoms. This parameter is expected to be affected by the support composition in the case of highly dispersed supported metal catalysts, as the ones studied in the present work, in addition to the composition and concentration of adsorbed reaction intermediate species. In fact, according to the He TPD and He TPSR experiments in the 25–225°C range on the Pt/Al<sub>2</sub>O<sub>3</sub> catalyst, the Pt surface adsorbs very little NO, if any, as opposed to the case of Pt/La<sub>0.5</sub>Ce<sub>0.5</sub>MnO<sub>3</sub> catalyst. Therefore, under the present reaction conditions the proposed mechanism for N<sub>2</sub> and N<sub>2</sub>O formation is associated with different kinetics on the present two supported Pt catalysts, each influenced by the oxidation state of Pt. It seems reasonable to suggest according to the H<sub>2</sub> TPSR results that in the case of Pt/Al<sub>2</sub>O<sub>3</sub> it appears that Pt can be more readily reduced by H<sub>2</sub> treatment than in the case of Pt/La<sub>0.5</sub>Ce<sub>0.5</sub>MnO<sub>3</sub> catalyst. This then allows the NO reduction by H<sub>2</sub> to completely proceed toward N<sub>2</sub> and H<sub>2</sub>O formation. The various N<sub>2</sub> peaks observed in the H<sub>2</sub> TPSR experiment on Pt/Al<sub>2</sub>O<sub>3</sub> in the 150–425°C range are due to reduction of NO that is spilled-over from the alumina support to the Pt surface. In the case of He TPSR experiment, part of this NO desorbs at very high temperatures due to decomposition reactions of the various nitrate and nitrito structures formed on the alumina support upon NO/H<sub>2</sub>/O<sub>2</sub> treatment of the catalyst at 140°C.

## 5. CONCLUSIONS

The following conclusions can be derived from the results of the present work:

(1) A 0.1 wt% Pt supported on La<sub>0.5</sub>Ce<sub>0.5</sub>MnO<sub>3</sub> (a mixed oxide containing LaMnO<sub>3</sub>, CeO<sub>2</sub> and MnO<sub>2</sub> phases) catalyst has proven to give the highest integral rate of NO conversion to N<sub>2</sub> (micromole per second per gram of Pt) during NO/H<sub>2</sub>/O<sub>2</sub> lean-NO<sub>x</sub> reaction in the 100–200°C low-temperature range ever reported in the open literature. A similar result has been obtained for the site reactivity,  $TOF_{\text{N}_2}$  (s<sup>-1</sup>) and N<sub>2</sub> selectivity parameters.

(2) The 0.1 wt% Pt/La<sub>0.5</sub>Ce<sub>0.5</sub>MnO<sub>3</sub> catalyst has shown also very high N<sub>2</sub> yields (>80%) in the presence of 5% H<sub>2</sub>O in the feed stream and for 20 h on stream. This performance is by far better than that exhibited by the 0.1 wt% Pt/Al<sub>2</sub>O<sub>3</sub> catalyst.

(3) A hydrogen-assisted NO dissociation step and a nitrogen-assisted mechanism for N<sub>2</sub> and N<sub>2</sub>O formation are proposed to explain the various NO TPD and TPSR experiments in He and H<sub>2</sub>/He flow following reaction in a satisfactory manner.

(4) The remarkable catalytic behavior of 0.1 wt% Pt/La<sub>0.5</sub>Ce<sub>0.5</sub>MnO<sub>3</sub> toward NO/H<sub>2</sub>/O<sub>2</sub> reaction is suggested to be due to various direct and indirect influences of support composition. In particular, oxygen vacant sites of support located next to the small Pt clusters could provide the means for the formation of adsorbed NO with the N atom located on the Pt metal and the O atom on the oxygen vacancy. Such an adsorbed state is expected to give rise to a higher rate of N<sub>2</sub> formation compared to the state of molecularly adsorbed NO on the Pt metal alone. In addition, adsorbed oxygen formed on the oxygen vacancies of support located at the metal–support interface could be considered to be more active in removing adsorbed hydrogen from the Pt surface. This result could regulate in the appropriate manner the surface coverage of adsorbed hydrogen toward activity and N<sub>2</sub> selectivity maximization.

(5) Deposition of 0.1 wt% Pt onto the Al<sub>2</sub>O<sub>3</sub> surface gives rise to a significant enhancement of NO adsorption on the Al<sub>2</sub>O<sub>3</sub> support at room temperature. This is very likely to be the result of a spillover phenomenon of NO from Pt to the support. The creation of new adsorption sites for NO on the metal–support interface can only partly account for this behavior.

(6) Two distinct adsorbed states of NO on the Pt/La<sub>0.5</sub>Ce<sub>0.5</sub>MnO<sub>3</sub> catalyst are observed to desorb in the 25–225°C range in He flow. Only the more strongly bound adsorbed state of NO was found to react with H<sub>2</sub> in the 25–225°C range.

(7) The surface coverage of adsorbed NH<sub>x</sub> ( $x=0-2$ ) species formed during NO/H<sub>2</sub>/O<sub>2</sub> reaction at 140°C was found to be very small compared to the surface coverage

of molecularly adsorbed NO on the Pt/La<sub>0.5</sub>Ce<sub>0.5</sub>MnO<sub>3</sub> catalyst.

### ACKNOWLEDGMENTS

Financial support by the Research Committee of the University of Cyprus is gratefully acknowledged. The experimental assistance of Chrystalla Charalambous (final year project student of this University) is also acknowledged.

### REFERENCES

- Fritz, A., and Pitchon, V., *Appl. Catal. B: Environ.* **13**, 1 (1997).
- Părvulescu, V. I., Grange, P., and Delmon, B., *Catal. Today* **46**, 233 (1998).
- Busca, G., Lietti, L., Ramis, G., and Berti, F., *Appl. Catal. B: Environ.* **18**, 1 (1998).
- Janssen, F. J., in "Handbook of Heterogeneous Catalysis" (G. Ertl, H. Knözinger, and J. Weitkamp, Eds.), p. 1633. VCH, Weinheim, 1997.
- Rausenberger, B., Swiech, W., Schmid, A. K., Rastomjee, C. S., Emgel, W., and Bradshaw, A. M., *J. Chem. Soc. Faraday Trans.* **94**(7), 963 (1998).
- Dumpelmann, R., Cant, N. W., and Trimm, D. L., in "3rd ICC and Automotive Pollution Control" (A. Frennet and J.-M. Bastin, Eds.). Vol. 2, p. 13. ULB Brussels, 1994.
- Tomishige, K., Asakura, K., and Iwasawa, Y., *J. Catal.* **157**, 472 (1995).
- Hecker, W. C., and Bell, A. T., *J. Catal.* **92**, 247 (1985).
- Hornung, A., Muhler, M., and Ertl, G., *Catal. Lett.* **53**, 77 (1998).
- Kobylinski, T. P., and Taylor, B. W., *J. Catal.* **33**, 376 (1974).
- Huang, S. J., Walters, A. B., and Vannice, M. A., *J. Catal.* **173**, 229 (1998).
- Burch, R., and Scire, S., *Catal. Lett.* **27**, 177 (1994).
- Salama, T. M., Ohnishi, R., Shido, T., and Ichikawa, M., *J. Catal.* **162**, 169 (1996).
- Tanaka, T., Yokota, K., Doi, H., and Sugiura, M., *Chem. Lett.* **273** (1997).
- Lindstedt, A., Strömberg, D., and Milh, M. A., *Appl. Catal.* **116**, 109 (1994).
- Ferri, D., Forni, L., Dekkers, M. A. P., and Nieuwenhuys, B. E., *Appl. Catal. B: Environ.* **16**, 339 (1998).
- Frank, B., Emig, G., and Renken, A., *Appl. Catal. B: Environ.* **19**, 45 (1998).
- Burch, R., and Coleman, M. D., *Appl. Catal. B: Environ.* **23**, 115 (1999).
- Ueda, A., Nakao, T., Azuma, M., and Kobayashi, T., *Catal. Today* **45**, 135 (1998).
- Yokota, K., Fukui, M., and Tanaka, T., *Appl. Surf. Sci.* **121/122**, 273 (1997).
- Burch, R., Millington, P. J., and Walker, A. P., *Appl. Catal. B: Environ.* **4**, 160 (1994).
- Fukui, M., Yokota, K., and Shokubai, K., *Catalysts Catal.* **36**, 160 (1994).
- Costa, C. N., Anastasiadou, T., and Efstathiou, A. M., *J. Catal.* **194**, 250 (2000).
- Eguchi, K., Kondo, T., Hayashi, T., and Arai, H., *Appl. Catal. B: Environ.* **16**, 69 (1998).
- Tejuca, L. G., Fierro, J. L. G., and Tascon, J. M. D., *Adv. Catal.* **36**, 237 (1989).
- Ari, H., and Tominga, H., *J. Catal.* **43**, 131 (1976).
- Solymosi, F., Bansagi, T., and Novak, E., *J. Catal.* **112**, 183 (1988).
- Srinivas, G., Chuang, S. S. C., and Debnath, S., *J. Catal.* **148**, 748 (1994).
- Busca, G., and Lorenzelli, V., *J. Catal.* **72**, 303 (1981).
- Burch, R., and Sullivan, J. A., *J. Catal.* **182**, 489 (1999).
- Hodjati, S., Vaezzadeh, K., Petit, C., Pitchon, V., and Kiennemann, A., *Appl. Catal. B: Environ.* **26**, 5 (2000).
- Eguchi, K., Watabe, M., Ogata, S., and Arai, H., *J. Catal.* **158**, 420 (1996).
- Klingenberg, B., and Vannice, M. A., *Appl. Catal. B: Environ.* **21**, 19 (1999), and references therein.
- Burch, R., Shestov, A. A., and Sullivan, J. A., *J. Catal.* **186**, 353 (1999).
- Odriozola, J. A., Heinemann, H., Somorjai, G. A., Garcia de la Banda, J. F., and Pereira, P., *J. Catal.* **119**, 71 (1989).
- Solymosi, F., and Knözinger, H., *J. Chem. Soc. Faraday Trans.* **86**(2), 389 (1990).
- Shustorovich, E., and Bell, A. T., *Surf. Sci.* **289**, 127 (1993).